Journal of Medicinal Chemistry Perspective

J. Med. Chem. **2010,** *53,* 3–17 **3**
DOI: 10.1021/jm9004708

Heat Shock Protein 90: Inhibitors in Clinical Trials

Marco A. Biamonte,*,† Ryan Van de Water,† Joseph W. Arndt,‡ Robert H. Scannevin,‡ Daniel Perret,† and Wen-Cherng Lee‡

†*Biogen Idec, 5200 Research Place, San Diego, California 92122, and* ‡*Biogen Idec, Cambridge, Massachusetts 02142*

Received April 12, 2009

1. Introduction

The function of the heat shock proteins (HSPs[a]) is to fold and maintain the proper conformation of other proteins, referred to as "clients". HSPs are therefore molecular chaperones. They are overexpressed when a cell is subjected to a transient increase in temperature or to other stresses, such as oxidants or radiations, to assist in refolding denatured client proteins.[1] In addition to mediating critical cellular stress responses, HSPs also play a routine homeostatic role in regulating client protein folding under nonstressed conditions.[2] Molecular chaperones are among the most abundant of cellular proteins, constituting 5−10% of all proteins in the cell,[3] including HSP90, which even under basal, nonstressed conditions comprises approximately 1% of the cellular protein population.[4]

HSP90 is the 90 kDa member of the family and exists as two isoforms: HSP90α is an inducible form overexpressed in cancer cells, while HSP90β is the constitutive form. Both HSP90α and HSP90β are found in the cytoplasm. There are also two paralogues: Grp94, localized in the endoplasmic reticulum lumen, and TRAP1, confined to mitochondria.

Inhibition of HSP90 causes client proteins to adopt aberrant conformations, and these abnormally folded proteins are rapidly eliminated by the cell via ubiquitination and proteasome degradation. Of the 280 reported HSP90 clients, 48 are involved in cell growth and various signaling cascades. Several HSP90 clients are notorious oncogenes (Raf-1, Akt, cdk4, Src, Flt-3, hTert, c-Met, etc.), and five are clinically validated cancer targets: HER-2/neu (Herceptin (trastuzumab)), Bcr-Abl (Gleevec (imatinib mesylate)), estrogen receptor (tamoxifen), androgen receptor (Casodex (bicalutamide)), and VEGF, the vascular endothelial growth factor receptor (Sutent (sunitinib)).[5−8]

Some client proteins are particularly responsive to HSP90 inhibitors and undergo rapid degradation at low concentrations of the inhibitor. The more sensitive clients are usually those involved in growth signaling, but some mutated proteins found in tumor cells (mutant p53, imatinib-resistant Bcr-Abl)[9] are also particularly dependent on HSP90 to preserve their conformation and function. The most sensitive client appears to be HER2 and is followed by mutant EGFR > Raf-1 > Akt > mutant BRAF > wild-type EGFR.[10]

Since inhibition of HSP90 can lead to the degradation of a large number of oncogenic proteins, HSP90 has become a target of interest for oncology. A major advantage of HSP90 inhibitors is that they simultaneously attack several pathways necessary for cancer development, reducing the likelihood of the tumor acquiring resistance to any single therapeutic pathway. It has also been proposed that HSP90 occurs in an activated form in cancer cells, whereas in normal somatic cells only the latent form is found. This has given rise to the hypothesis that HSP90 inhibitors could be designed to selectively target the activated form and thus more specifically target cancer cells,[11,12] but this assertion has been challenged.[13] Furthermore, the activity of HSP90 is regulated by proteins called cochaperones, and tumor cells, which have higher levels of given cochaperones, exhibit higher levels of HSP90 activity compared to noncancerous cells.[11,14]

It has been debated if HSP90, being implicated with so many clients, could provide an acceptable therapeutic index. Empirical evidence supports the pursuit of HSP90 inhibitors. Cancer cells seem to have a higher HSP90 activity than normal cells, and oncogenes are more dependent on HSP90 than house-keeping proteins. In cell cultures, HSP90 inhibitors kill tumor cells at concentrations much lower than those required to kill normal cells. In mice, efficacy can be observed at nontoxic doses, and in humans, the first signs of clinical benefit are emerging. It remains to be verified, however, if HSP90 inhibitors will truly provide a sufficient safety margin in the clinic.

2. Assays

To exert its function, HSP90 needs to bind ATP in a pocket located in the N-terminal domain. The natural product geldanamycin (Figure 1, **1**) and all the inhibitors discussed herein bind to that same pocket. Since geldanamycin was the first HSP90 inhibitor discovered, binding assays have typically relied on monitoring the displacement from HSP90 of a geldanamycin-based probe, usually a fluorescently labeled version of geldanamycin.[15,16] It has only recently come to light that geldanamycin and its derivatives exist in vivo in both

*To whom correspondence should be addressed. Phone: (858) 401-5082. Fax: (858) 795-9642. E-mail: marco.biamonte@biogenidec.com.

[a] Abbreviations: ADP, adenosine diphosphate; AML, acute myeloid leukemia; AMP-PNP, adenylyl imidodiphosphate; ATP, adenosine triphosphate; AUC, total area under the drug concentration−time curve; C_{max}, maximum plasma drug concentration during a dosing interval; Cl, total clearance of drug in plasma; CLL, chronic lymphocytic leukemia; DTT, 1,4-dithio-DL-threitol; EPL, egg phospholipid; FDG, 2-fluoro-2-deoxy-D-glucose; FP, fluorescence polarization; GIST, gastrointestinal stromal tumors; HSP, heat shock protein; MTD, maximum tolerated dose; NCI, National Cancer Institute; NHL, non-Hodgkin's lymphoma; NSCLC, non-small-cell lung cancer; PET, positron emitted tomography; PGP, P-glycoprotein; PMSE, phospholipon−miglyol−soybean oil emulsion; RECIST, response evaluaton criteria in solid tumors; T_{max}, time after dosing when at maximum plasma drug concentration; TCEP, tris(2-carboxyethyl)phosphine; TFAA, trifluoroacetic anhydride; TGI, tumor growth inhibition; V, volume of distribution.

Published on Web 09/16/2009

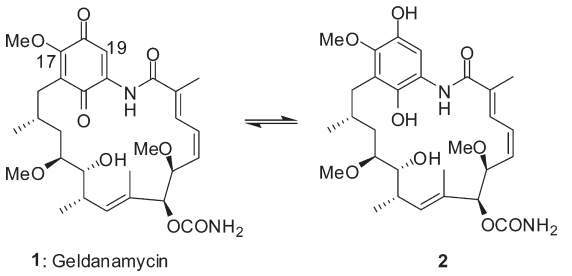

Figure 1. Geldanamycin in equilibrium between the quinone and hydroquinone forms.

the quinone (**1**) and the hydroquinone (**2**) forms, with the latter binding HSP90 much more tightly (0.05 vs 2 μM).[17] Controlling the redox state of the binding assay is therefore critical to obtain accurate and meaningful binding data. This can be done by incorporation of a reducing agent such as 1,4-dithio-DL-threitol (DTT; see below). The effect of the quinone reduction, now demonstrated in multiple assay formats, needs to be reconciled with previous literature data. Binding data obtained prior to 2004 typically do not incorporate a reducing agent and if so are probably unreliable.

Fluorescence polarization (FP) assays have come to the forefront as a convenient format in which to screen potential HSP90 inhibitors.[13,18−21] They offer the advantage of being "mix and read" homogeneous assays that are amenable to high-throughput compound screening.[18] These assays utilize fluorescently labeled derivatives of geldanamycin and monitor the reduction of polarization when competitive inhibitors are present and displace the fluorescent geldanamycin probe on HSP90. As alluded to above, controlling the redox state of the assay has proved to be essential, since the geldanamycin-based probes bind more tightly when they are in their hydroquinone form. Howes et al.[19] reported binding constants of 281 nM for geldanamycin (**1**) and 1270 nM for 17-allyl-17-desmethoxygeldanamycin (17-AAG, **3**); however, reducing agents were not included in the assay buffers. Gooljarsingh et al.,[13] Du et al.,[18] Kim et al.,[20] and Onuoha et al.[21] all described a time-dependent improvement in binding affinity of fluorescently labeled geldanamycin for HSP90. A commonality in these assays was the inclusion of a reducing agent (typically DTT, 1,4-dithio-DL-threitol) in the assay buffer so that over time the assay constituents were reduced. The effect of reduction was thoroughly examined in this assay format by Onuoha et al.[21] in which preincubation of the fluorescent geldanamycin probe with the reducing agent TCEP (tris-(2-carboxyethyl)phosphine) abolished the time-dependent effect on binding and revealed high affinity for HSP90 even with short incubation times. Onuoha et al.[21] also demonstrated that in the absence of reducing agents, the binding did not increase with time, and low affinity binding was observed even with 24 h incubation times.

Functional, cell-based assays provide additional information, since they take into account the effects of HSP90 cochaperones that are not present in recombinant protein binding assays and add additional compound selection filters such as cell permeability. Furthermore, if the cell-culture medium contains serum proteins, protein-binding effects are implicitly taken into account. One such assay monitors the effect of HSP90 inhibitors on the degradation of the HSP90 client HER2 in breast-cancer MCF7 cells. HER2 is a receptor located on the surface of cells, and its expression can be easily monitored with extracellular-directed fluorescent antibodies and flow cytometry. We have found this assay to be reliable and reproducible.[22] In summary, the combination of a binding assay and a cell-based assay offers the best assessment of HSP90 inhibitors in vitro.

3. Design and Synthesis of HSP90 Inhibitors

Of the 12 HSP90 inhibitors that are in clinical trials, the structures of the following 6 have been disclosed (Figure 2): 17-allylamino-17-desmethoxygeldanamycin (17-AAG, **3**)[23] and its hydroquinone (IPI-504, **4**),[24] 17-(dimethylamino-ethylamino)-17-desmethoxygeldanamycin (17-DMAG, **5**),[25] the purine BIIB021 (**6**),[26] the resorcinol NVP-AUY922 (**7**),[27] and the benzamide SNX-5422 (**8**),[28] a glycine prodrug of SNX-2112 (**9**). At the time of writing, it appears that there are six additional compounds in clinical trials, but their structures have not been made public. We now give a brief overview of the design of inhibitors **3**−**9**.

3.1. 17-AAG, Oxidized Form (3). Ansamycins **3**−**5** are all derived from geldanamycin (**1**), which was first isolated in 1970 by scientists at Upjohn by fermentation of *Streptomyces hygroscopicus*.[29,30] The structure of geldanamycin was elucidated 1 year later.[31] Geldanamycin was originally of interest for its antibiotic properties, but the high reactivity of the 17-MeO group made it unsuitable for drug development. The 17-MeO group is easily displaced with amines at room temperature, and treatment of geldanamycin with allylamine provides the more stable 17-AAG quantitatively in less than 1 h. 17-AAG was first reported in 1980 in a patent application by Kaken Chemicals, Tokyo, claiming its antitumor properties,[32]and later in 1995 by Pfizer.[23] Initially, the activity of 17-AAG was poorly understood, and 17-AAG was mistaken to be an inhibitor of the HER2 kinase. Only after 1994 was 17-AAG recognized to actually inhibit HSP90, thereby inducing HER2 degradation and giving the erroneous impression of direct inhibition of HER2.[33,34] 17-AAG entered clinical trials in 1999.

3.2. 17-AAG, Reduced Form (4). 17-AAG is notoriously insoluble and difficult to formulate. As mentioned earlier, 17-AAG is partially converted in vivo to its hydroquinone form, which also inhibits HSP90 effectively. Infinity Pharmaceuticals reduced 17-AAG with $Na_2S_2O_4$ and isolated the resulting hydroquinone as the HCl salt **4**, which is far more water-soluble than the parent 17-AAG (250 vs. 0.02 mg/mL, respectively). The hydrochloride **4** is stable at −20 °C but not at room temperature.[24] It entered clinical trials in January 2005.

3.3. 17-DMAG (5). Another way to increase the solubility of the geldanamycin analogues was to attach an ionizable amino group. 17-DMAG (**5**), the *N*,*N*-dimethylethylamino analogue of 17-AAG, proved to be potent and to have improved water solubility. Kosan put 17-DMAG in clinical trials in August 2006 but discontinued it in 2008 to "commit resources to the development of 17-AAG for the treatment of breast cancer as a result of a comparative analysis with 17-AAG based on several factors, including clinical experience to date, strength of intellectual property protection and risk, and time to commercialization".[35]

3.4. Purine 6. Using structure-based drug design, researchers at the Memorial Sloane Kettering Institute developed chimeric molecules by purposely combining the structural aspects of ATP (adenine ring) and 17-AAG (aromatic ring), which led to the discovery of PU3 (**10**, Figure 3), the first fully synthetic inhibitor of HSP90.[36] The weakly active **10**

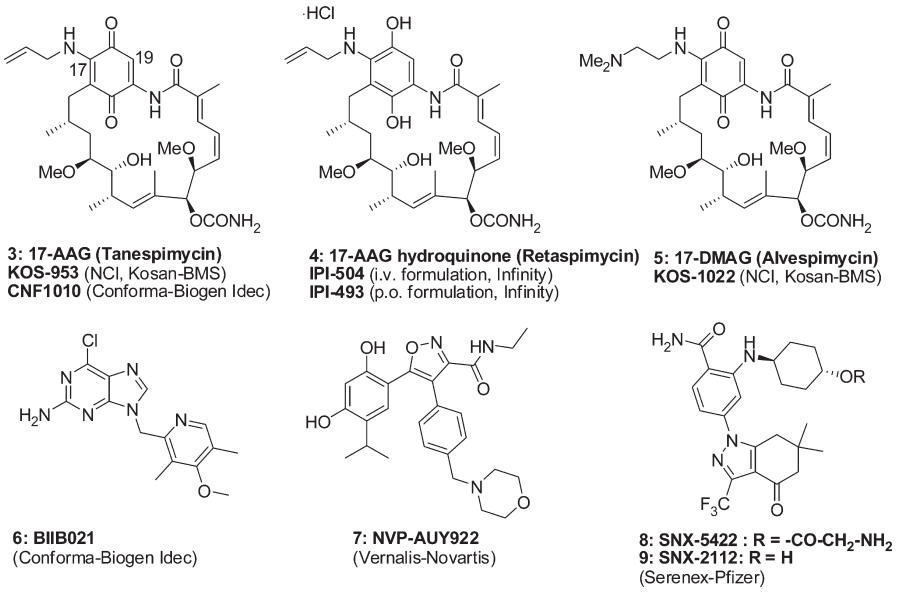

Figure 2. Six HSP90 inhibitors in clinical trials of which the structures have been disclosed.

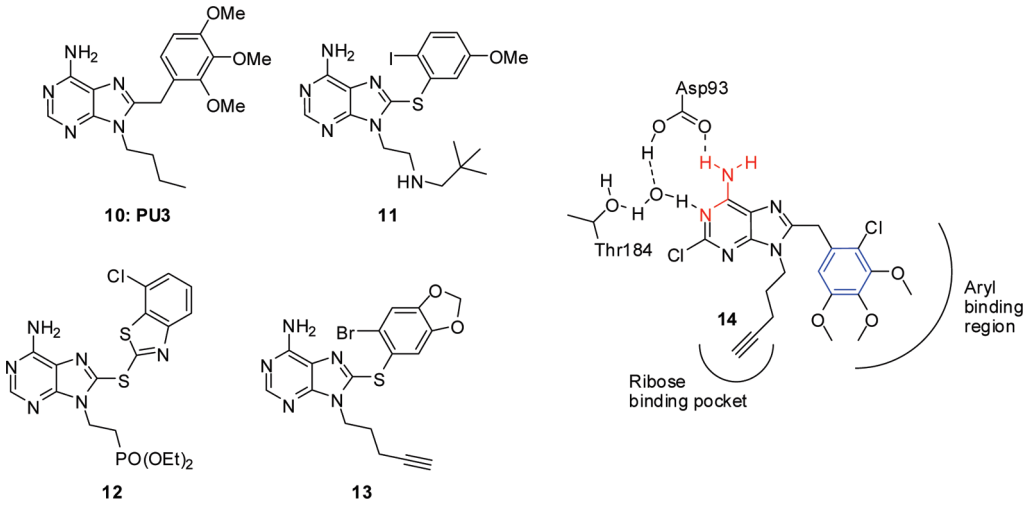

Figure 3. Early synthetic inhibitors of HSP90 and proposed pharmacophore.

(40 μM in a HER2 degradation assay) was optimized independently by Conforma Therapeutics[37−39] (**11**, **12**) and Memorial Sloan-Kettering Institute[40] (**13**) to give compounds with potencies ranging from 30 to 100 nM in the HER2 degradation assay. Compounds **11**−**13** are also orally active, contrary to 17-AAG, but high doses are required for efficacy in xenograft models (>100 mg/kg).

Although compounds **11** and **12** were not sufficiently potent to be further developed, they served to establish a pharmacophore model highlighting two key features, illustrated with compound **14** (Figure 3): (1) a NH_2−C=N fragment able to bind the purine pocket of HSP90, thus mimicking the NH_2−C=N fragment of ATP and (2) an aromatic ring located exactly six bonds away (5 Å) from the NH_2 group. In addition, a purine scaffold, rich in basic nitrogen atoms and offering multiple possibilities for hydrogen bonding, also seemed to be necessary.

On the basis of this pharmacophore model, the two key features were "rotated" around the purine ring to give the new guanine series **16** (Figure 4). Series **16** preserves the 5 Å distance (6-bonds) between the NH_2 and the aryl group, but

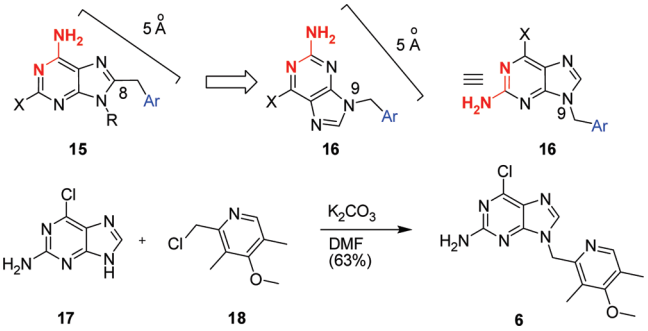

Figure 4. Pharmacophore hypothesis (**15**), transposition of key binding elements to generate a new series (**16**), and synthesis of clinical candidate **6** (Conforma-Biogen Idec).

the aryl group is connected to the scaffold via N-9 rather than C-8. This connectivity notably simplified the synthesis of the new series, which culminated with the discovery of **6**, assembled in a single step from inexpensive commercial reagents (Figure 4).[26] Purine **6** entered clinical trials in 2005 as an oral drug for hematological and solid tumors.

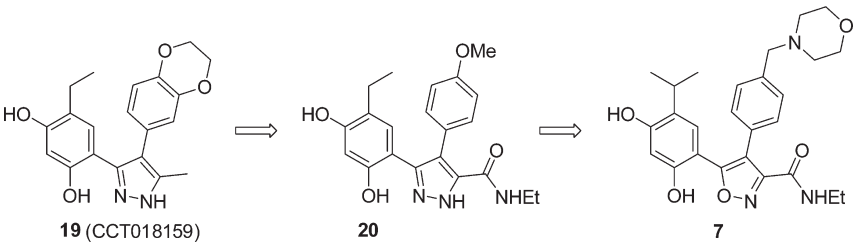

Figure 5. Lead evolution of clinical candidate **7** (Vernalis-Novartis).

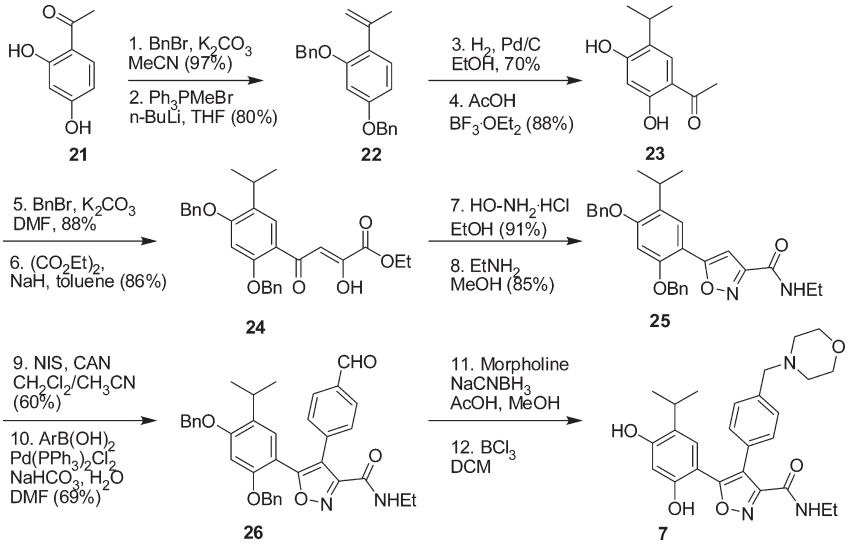

Figure 6. Synthesis of clinical candidate **7** (Vernalis-Novartis).

3.5. Resorcinol 7. Researchers at Vernalis (which started a collaboration with Novartis in 2004) adopted a structure-guided approach in designing HSP90 inhibitors. Vernalis screened for compounds able to bind HSP90 and identified as a starting point resorcinol **19** (Figure 5), a motif also found in the natural product and HSP90 inhibitor radicicol (see later, **39**). Further optimization led to **20**, where the amide group was key in forming a new interaction with the protein (Gly97).[41] Finally, introduction of a solubilizing group and minor structural modifications led to the clinical candidate **7**.[27] The medicinal chemistry route was a 12-step synthesis (Figure 6). Resorcinol **7** entered clinical trials in September 2007 as an intravenous infusion.

3.6. Benzamide 8 and Its Active Metabolite 9. To identify HSP90 inhibitors, Serenex (acquired by Pfizer in 2008) has developed an ATP-affinity column. When cell lysates were loaded on the column, approximately 2000 ATP-binding proteins were captured. Using a mass spectrometry platform, Serenex screened for compounds that would selectively displace HSP90 from the column and identified compounds **27**, **28**, and the benzamide **9** (Figure 7). Benzamide **9** has variable oral bioavailability and produces polymorphic crystal forms unsuitable for development.[42] These issues were resolved with the glycine prodrug **8**. Prodrug **8** has been in clinical trials since May 2007 as an oral inhibitor of HSP90. The medicinal chemistry route for preparing benzamide **9** involves five steps.[28]

3.7. Other Inhibitors. The structures of the six other clinical HSP90 inhibitors have not been disclosed yet. Of note, however, is the work of Kyowa Hakko and Biotica Technology. 17-AAG is known to be hepatotoxic, an effect that has been ascribed to its quinone ring reacting at C-19 with glutathione under physiological conditions ($T_{1/2}$ = 9.8 h for 17-AAG, 26 min for 17-DMAG).[43] Kyowa Hakko prepared geldanamycin derivatives devoid of quinones by reacting 17-AAG and analogous quinones (Figure 8, **35**) with MeMgBr, followed by $Zn(BH_4)_2$ to obtain 4-methylphenol derivatives of type **36**.[44] Biotica Technology focused on the HSP90 inhibitor macbecin (**37**) and genetically engineered the microorganism that secretes it, *Actinosynemma pretiosum*.[45] Deletion of the genes responsible for the C-21 monooxidation and the four susbequent biosynthetic steps (C4,5-desaturation, C15-hydroxylation, and C11/C15-O-methylation) yielded a new strain that produced exclusively phenol **38** at > 200 mg/L. Phenol **38** (K_d = 3 nM) had in mice a "therapeutic index" 3 times higher that 17-AAG, suggesting that the quinone ring of 17-AAG is indeed responsible for toxicity.[45]

Several years earlier, in 1996, Kyowa Hakko disclosed another natural product, radicicol (**39**), and its oxime derivatives (**40**),[46,47] but did not pursue further clinical studies. Finally, efforts directed at finding novel HSP90 inhibitors have been thoroughly reviewed elsewhere.[48]

4. Structural Biology of HSP90 and Comparison of Ligand Binding Modes

The activity of HSP90 is regulated by a sophisticated process that involves HSP90 dimerization, ATP/ADP binding and hydrolysis, and formation of complexes with cochaperones. In cells, HSP90 is present as a dimer. Crystal structures of several full length HSP90s, from yeast, *E. coli*, and an endoplasmic reticulum paralogue, have been solved, and their structural biology has been recently reviewed.[2,49−52] HSP90s

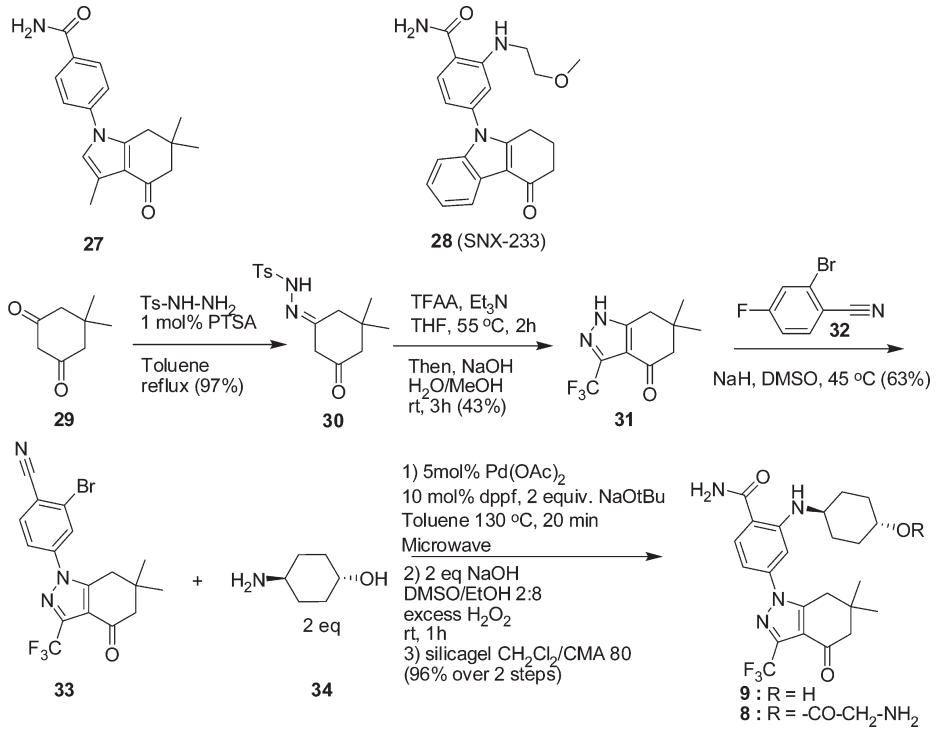

Figure 7. Early Serenex HSP90 inhibitors **27** and **28** and synthesis of **9**, the active metabolite of clinical candidate **8** (Serenex-Pfizer).

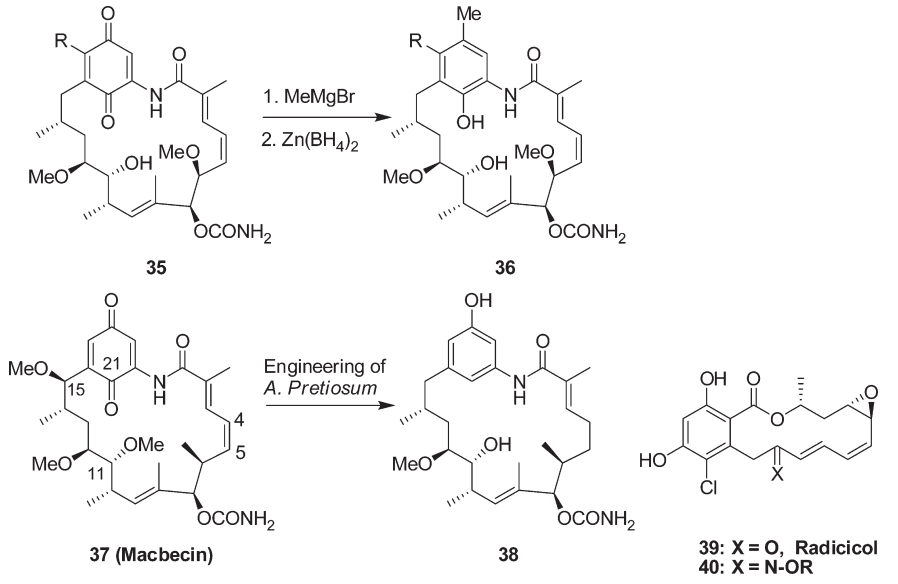

Figure 8. Other inhibitors of HSP90.

share a common architecture and are divided into three functional domains (Figure 9A): (a) an N-terminal domain that comprises an ATP-binding pocket,[53] (b) a middle domain that regulates the interaction with substrate client proteins and also contains residues critical for ATPase activity,[54,55] and (c) a C-terminal domain that regulates HSP90 dimerization and contains a second nucleotide-binding site.[56,57] The binding of ATP, its hydrolysis, and the resultant ADP binding drive a series of conformational changes in the N-terminal domain ATP lid (Figure 9B).[49,58] The structure of the entire dimer is affected, and the hydrophobic faces of HSP90 shift from an open conformation able to bind a client protein to one in which they get buried internally, thereby facilitating client release.

Beyond complex intramolecular conformational changes, HSP90 exerts its functional activity in vivo through the interactions with cochaperone molecules, of which over a dozen have been identified (Figure 10). The cochaperones HSP70 and HSP40 are both required for loading client proteins on HSP90 and for substrate maturation,[59] and their interaction is regulated via the action of Hop/Sti1.[60] Other cochaperones such as Hip, Aha1, and Cdc37 are also present in the pre-ATP-bound HSP90−client complex. Upon binding of ATP, these cochaperones are dissociated from the HSP90 complex and are replaced by others, such as p23/Sba1 and immunophillins, to form the mature refolding complex. Upon release of the client, the mature complex is dissociated so the

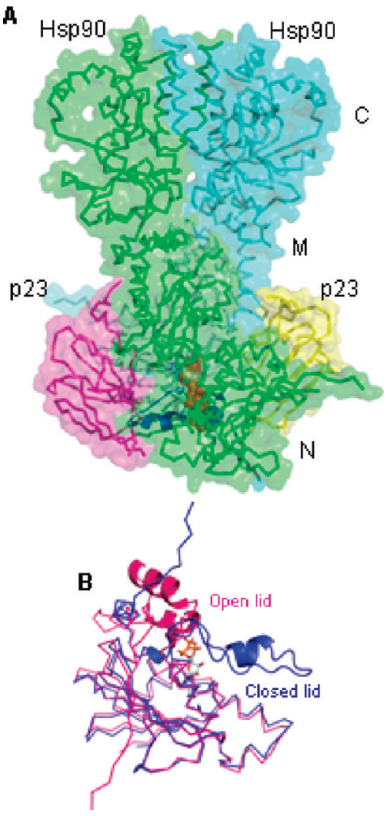

Figure 9. (A) Crystal structure of the yeast HSP90 dimer, in complex with p23/Sba1. Nonhydrolyzable ATP analogue is in red: N = N-terminal domain; M = middle domain; C = C-terminal domain. (B) Close-up of ATP-driven lid closure in N domain.

chaperone sequence can recycle and bind new client proteins. When an inhibitor such as geldanamycin is bound in the HSP90 ATP-pocket, the cycle is interrupted and the misfolded client is tagged with ubiquitin via the action of Hip and flagged for degradation by the 26S proteasome. Hip binds to HSP70[61] and HSP90[62] and appears to be an E3 ligase responsible for ubiquitinylation of client proteins.[63,64] Hip can also activate the release of the transcription factor HSF1, which turns on the cellular stress response and protects against programmed cell death.[65]

The number of X-ray crystal structures of HSP90 has increased dramatically with presently over 100 HSP90 structures in the Protein Data Bank. They include apo and binary complexes with ADP, the ATP-analogue AMP-PNP (adenylyl imidodiphosphate), small-molecule inhibitors, and protein−protein complexes with cochaperones. Comparisons of the binding modes of the inhibitors and of ADP reveal certain common features (Figure 11). For instance, examination of the purine binding pocket of the ADP cocrystal structure (Figure 11A) exposes two critical hydrogen bonds: the first one is observed between the NH_2 group of adenine and residue D93, and the second is observed between N-1 of adenine and T184 via a bridging water molecule (Figure 11A).[66] Interestingly, the hydrogen bonds with D93 and T184 are conserved features with all the known HSP90 inhibitors, including 17-AAG and its analogue 17-DMAG (Figure 11B),[16] the resorcinol containing moieties of radicicol (Figure 11C) and Novartis-Vernalis resorcinol **7** (Figure 11E),[67] the purine scaffold of **10** (Figure 11D), and carbazolone **28**, an analogue of Serenex-Pfizer benzamide **9** (Figure 11F).

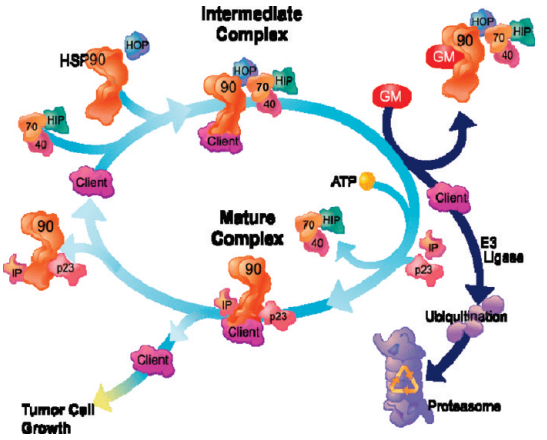

Figure 10. HSP90 cycle: GM = geldanamycin analogue; 40 = HSP40; 70 = HSP70; IP = immunophillin; HIP = HSP70-interacting protein; HOP = HSP70/HSP90 organizing protein. Cdc37 and Aha1 are not shown.

Nonetheless, important disparity in how these HSP90 inhibitors bind to the ATP-binding cleft also exists. For example, in the 17-DMAG cocrystal structure, the N106 that interacts with the sugar of ADP is pushed out of the active site to accommodate the methoxy moiety (Figure 11B). The loss of this interaction is more than offset by several additional H-bonds that are picked up between K58 and a hydroxyl, between the K112 and a quinone oxygen, and between the G135 carbonyl and the cis amide nitrogen of 17-DMAG.[16] While the Novartis-Vernalis resorcinol **7**[67] and radicicol (**39**) share similarity in their active site binding footprint, an additional H-bonding interaction with the C-5 ethylamide residue of **7** with G97 is not seen in the radicicol cocrystal structure (Figures 11C,E). It was shown that the ethylamide is critical to gain additional potency. Furthermore, Serenex-Pfizer benzamide **9** is expected to bind as in the published crystal structure of the related tetrahydro-4*H*-carbazol-4-one **28** (PDB code 3d0b) which makes additional hydrophobic interactions with the aryl binding pocket formed by L103, L107, F138, V150, and W162 of HSP90.[68] This binding mode resembles that seen for 8-benzylpurine **10** in which L107 and its associated helix are displaced by the trimethoxybenzyl moiety of **10**, inducing it into an extended helix conformation. Interestingly, several distinct structural conformations have been observed in this region of HSP90 involving residues 104−111 (Figure 12).[69] This area of HSP90 has been shown to unwind to form open, closed, or intermediate conformations, as seen in the cocrystal structures of ADP, 17-AAG, radicicol, Vernalis' resorcinol **7**, and Vernalis' naphthalene **41** (a preclinical inhibitor, PDB code 2bz5, Figure 13), indicating considerable plasticity in this region of the structure.

5. Preclinical Biological Data and Clinical Data

Table 1 summarizes the binding data and cell-based activities of the clinical inhibitors and of 17-AG, an active metabolite of 17-AAG. All the compounds have similar potencies in the HER2 degradation assay, with IC_{50} values ranging from 7 to 35 nM. This section describes the preclinical data of each inhibitor.

5.1. Geldanamycin Analogues. 17-AAG binds HSP90 with an affinity of the order of 500 nM as the quinone form and 9 nM as the hydroquinone form (Table 1). When incubated with MCF7 breast-cancer cell lines, 17-AAG induces HER2

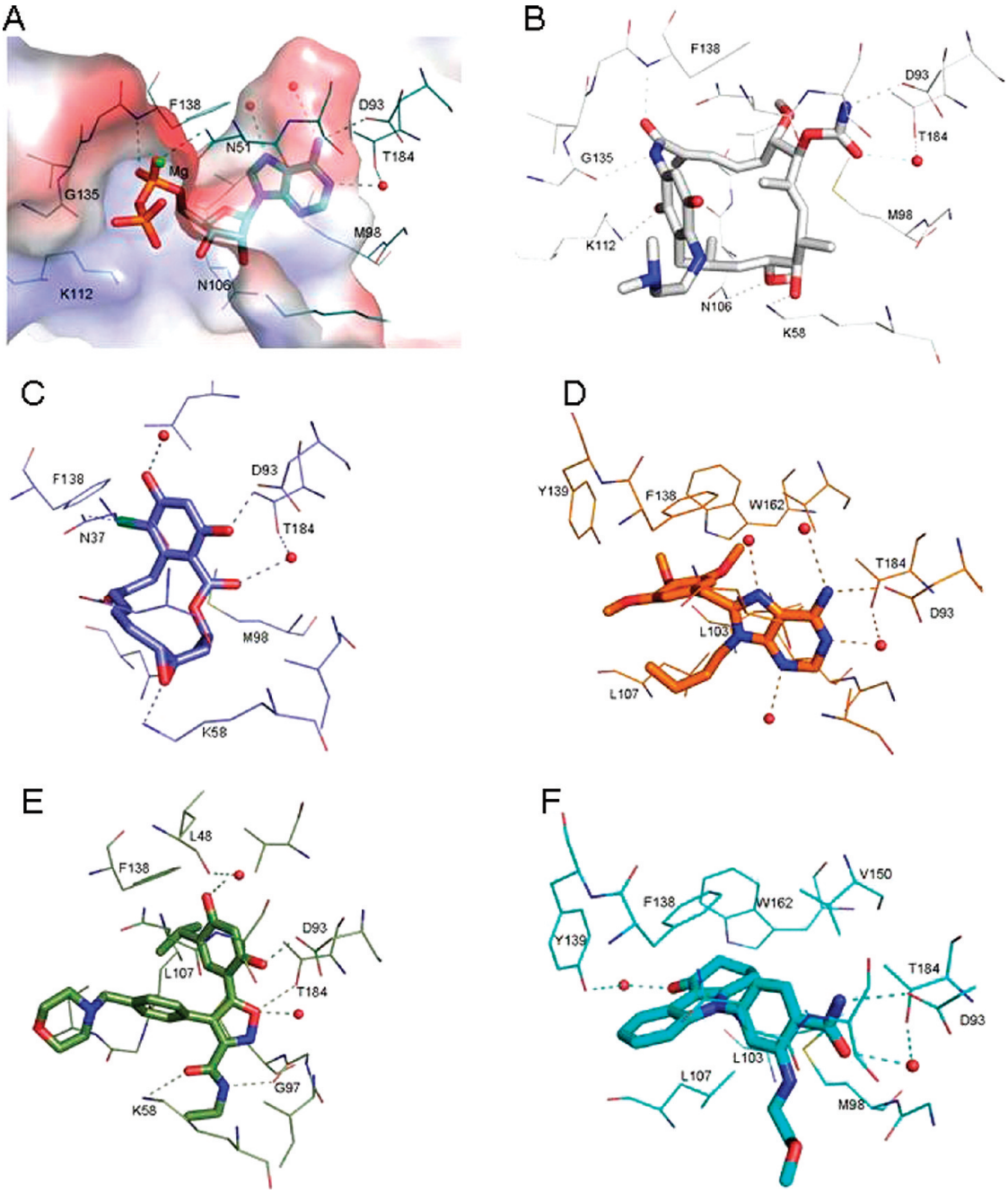

Figure 11. Comparison of HSP90 inhibitor binding modes: (A) ADP (carbon atoms in teal, PDB code 1byq) superimposed on active site electrostatic surface representation; (B) 17-DMAG (carbon atoms in white, PDB code 1osf); (C) radicicol (**39**) (carbon atoms in slate blue, PDB code 1bgq); (D) purine **10** (carbon atoms in orange, PDB code 1uym); (E) resorcinol **7** (carbon atoms in light green, PDB code 2vci); (F) compound **28**, an analogue of benzamide **9** (carbon atoms in cyan, PDB 3d0b). Active site water molecules (red spheres) and hydrogen bonds (dashes) are also indicated.

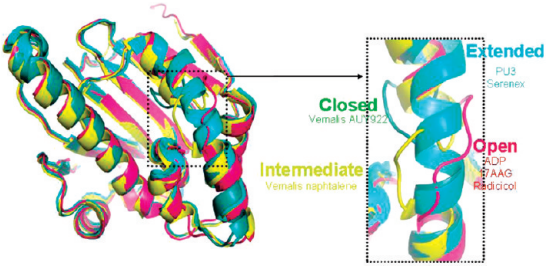

Figure 12. Conformational flexibility observed in HSP90 N-terminal domain.

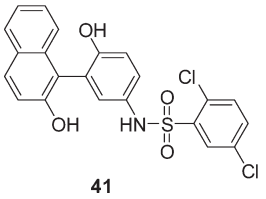

41

Figure 13. Vernalis preclinical inhibitor **41**.

degradation with an IC_{50} of 12 nM. 17-AAG also degrades other client proteins and up-regulates HSP70, while non-clients (e.g., PI3K) remain unaffected, a signature of HSP90

Table 1. Binding Constants and HER2 Degradation Values

inhibitor	K_i [nM][a] reducing conditions (+TCEP)	K_i [nM][a] nonreducing conditions (−TCEP)	HER2 degradation[b] [nM]
17-AAG	9.0 ± 4.7	530 ± 170	12 ± 5
17-AG	3.0 ± 1.8	21 ± 8	12 ± 3
6	13 ± 3.5	26 ± 18	38 ± 10
7	0.064 ± 0.058[c]	0.069 ± 0.047[c]	7 ± 1
9	1.1 ± 0.4	2.8 ± 2.1	22 ± 3

[a] All K_i values from Infinity.[70] [b] All HER2 degradation values from Biogen Idec.[22] [c] Note that the laboratory that developed 7 reports for its own compound a substantially different K_i = 9 nM.

inhibition. Note that HSP70 protects cells against insults. Thus, induction of the cytoprotective HSP70, an unavoidable side effect of HSP90 inhibition, is somewhat counterproductive because HSP90 inhibitors are meant to damage cancer cells.[71] Inhibition of HSP90 also leads to a slight HSP90 upregulation. The up-regulation of HSP70 (and to a lesser extent of HSP90) has caused concerns that it would be challenging to maintain an effective dosing schedule in the clinic.

Importantly, 17-AAG is a P-glycoprotein substrate and is less effective in PGP expressing tumor cell lines. Loss of the NQ01 gene, which is required for the bioreduction of 17-AAG to the more potent hydroquinone form, has also been proposed to be a mechanism of resistance. In cells, 17-AAG works in synergy with other cancer therapeutics, such as paclitaxel (Taxol, in a sequence-dependent manner),[72,73] cisplatin,[74] bortezomib (Velcade),[75] and trastuzumab.[76] In vivo, 17-AAG is rapidly metabolized to not only 17-desmethoxy-17-aminogeldanamycin (17-AG) but also acrolein, thus making it a dubious choice for a therapeutic agent. It is noted that the metabolite 17-AG is essentially as potent as its parent 17-AAG.

The pharmacokinetic properties of 17-AAG were examined by administering the compound in a DMSO/egg phospholipid formulation to A2780 tumor-bearing mice, ip, at 80 mg/kg.[77] Over the first 3 h, 17-AAG accumulates in the liver (liver/plasma ≈ 10) but not in the tumor (tumor/plasma ≈ 0.5). However, 17-AAG is retained for over 24 h in the tumor, while it is cleared rapidly from plasma and liver (other organs not reported). Additional parameters are given in Table 2. The half-life of 17-AAG is 0.9 h in plasma and liver but is 7.5 h in the tumor. The metabolite 17-AG behaves similarly, with short half-lives in plasma and liver (1.2 and 1.8 h, respectively) and longer half-lives in the tumor (13 h).

In xenograft models, with the same DMSO/egg phospholipid formulation, 17-AAG is administered to mice typically ip at 80 mg/kg twice weekly, leading to tumor growth inhibition of about 70−90%.[77] Synergistic effects between 17-AAG and paclitaxel have been noted in vivo.[10,73] In gefitinib-resistant EGFR (epidermal growth factor receptor) xenograft models, the combination of 17-AAG and paclitaxel was significantly more effective than either drug alone. While the drugs given individually inhibited tumor growth by ∼50%, the combination gave partial regressions.[10] Note that mutated forms of EGFR are highly sensitive to HSP90 inhibition and are found in 10−25% of the nonsmall cell lung cancers.

The clinical trials involving 17-AAG have been recently reviewed.[78] A central theme with 17-AAG is its lack of solubility, which led to increasingly sophisticated formulations. The first formulation was introduced in 1999 by the NCI and consisted of a DMSO/egg-phospholipid vehicle for intravenous administeration. In a phase I study, only minimal efficacy was observed and hepatoxicity (transaminitis) did occur. In addition, the DMSO caused anorexia and odors of dimethyl sulfide in patients.[78] The maximum tolerated dose (MTD) was schedule dependent, ranging from 56 mg/m^2 on a daily basis to 220 mg/m^2 when given every 3 days (a 70 kg human being corresponds to 2 m^2). On daily dosing, hepatic toxicity was dose limiting, and intermittent schedules were recommended.[79] The human PK parameters (Table 3) indicate that at 220 mg/m^2 17-AAG gave an initial C_{max} = 7.5 μM that exceeded the cell-based potency (HER2 degradation IC_{50} = 12 nM). 17-AAG had a $T_{1/2}$ of 3.8 ± 2.2 h (4 times longer than in mice) and was rapidly cleared with Cl = 42 L/h (human hepatic blood flow = 90 L/h). The active metabolite 17-AG was present in equal amounts as 17-AAG, based on the plasma AUC (∼22 μM·h).[79] An independent work gave similar parameters.[80]

Table 2. Mouse PK Parameter of 17-AAG Administered ip, 80 mg/kg, in DMSO/Egg Phospholipid

analyte	tissue	C_{max} [μM]	AUC [μM·h]	V_z [L]	Cl [L/h]	$T_{1/2}$ [h]
17-AAG	plasma	35	68	0.05	0.04	0.88
17-AAG	tumor	15	80	0.34	0.03	7.5
17-AAG	liver	126	263	0.01	0.01	0.86
17-AG	plasma	4.8	15	0.18	0.11	1.2
17-AG	tumor	3.5	43	0.49	0.03	13.7
17-AG	liver	18	59	0.06	0.02	1.8

Table 3. Human Pharmacokinetic Parameters of 17-AAG, Administered at a Dose of 220 mg/m^2 in DMSO/Egg Phospholipid[a]

analyte	C_{max} [μM]	T_{max} [h]	$T_{1/2}$ [h]	AUC [μM·h]	Cl [L/h]	V_{dss} [L]
17-AAG	7.5 ± 3.3		3.8 ± 2.2	22 ± 10	42 ± 20[b]	140 ± 60[c]
17-AG	3.0 ± 1.2	1.7 ± 0.5	6.9 ± 4.3	21 ± 13		230 ± 110[c]

[a] All values from Solit et al.[79] except where noted. [b] The clearance was converted from (L/h)/m^2 to L/h assuming patients of 2 m^2. [c] Value from Banerji et al.[80]

In spite of the rapid clearance of 17-AAG in humans, its pharmacodynamic effects lasted for at least 24 h, as judged by c-Raf-1 inhibition, cdk4 depletion, and HSP70 induction in peripheral blood leukocytes.[80] This illustrates an important point pertaining to HSP90 inhibitors. Though they may be short-lived, they rapidly induce the degradation of the relevant clients and the cell requires 24−48 h to resynthesize them. A continuous inhibition of HSP90 is therefore not necessary, and compounds with short half-lives can provide a long-lasting pharmacodynamic effect.

Kosan Pharmaceuticals developed a DMSO-free formulation of 17-AAG (KOS-953).[81] The Kosan formulation contained cremophor, which can induce hypersensitivity reactions and anaphylaxis and requires premedication with antihistamines and steroids. Patients were treated with up to 450 mg/m^2 of drug on a weekly schedule, and the dose was limited not because of toxicity but because of constraints on volume and formulation.[82] Importantly, the combination of 17-AAG and trastuzumab induced regressions of 21−25% in HER2 positive breast tumors, even if patients had failed trastuzumab therapy. These are some of the strongest clinical data supporting 17-AAG. Equally significant is that multiple myeloma patients, even if refractory to bortezomib, still responded to the combination of bortezomib and 17-AAG.[83] Responses were also observed in metastatic melanoma.

The cremophor-based formulation has recently been modified to an injectable suspension that does not require steroid premedication.[78]

Conforma Therapeutics developed an oil-in-water nanoemulsion of 17-AAG (CNF1010). Clinical trials were initiated in 2005. This oil-in-water formulation of 17-AAG is not currently pursued by Biogen Idec.[84]

Infinity Pharmaceuticals formulated 17-AAG in its hydroquinone form, trapped as a HCl salt (**4**). This makes sense, since 17-AAG is in equilibrium with its reduced hydroquinone in vitro (liver microsomes) and in vivo. For instance, iv injection of 17-AAG to mice leads to 5 times more hydroquinone than 17-AAG. In xenograft models, **4** is typically dosed iv at 100 mg/kg (300 mg/m^2) twice weekly and induces tumor growth inhibitions on the order of 70%. Coadministration of bortezomib at 0.3 mg/m^2 iv had a synergistic effect and led to 100% TGI.[85] Hydroquinone **4** entered clinical trials in 2005 and gave promising results in gastrointestinal stromal tumors (GIST) on a twice weekly schedule (400 mg/m^2).[86] Positron emitted tomography (PET) imaging was performed with 18-fluorodeoxyglucose to measure the metabolic activity of the tumors. Fifteen of 18 patients achieved stable diseases, and four partial responses were observed. This study prompted a phase III trial in GIST, which was initiated in August 2008. The trial was suspended when safety data from the first 46 patients enrolled in the study showed a higher than anticipated mortality rate. A preliminary review of the data suggests that the patients had more advanced disease, as evidenced by a greater percentage of patients having received three or more prior therapies and longer time since initial diagnosis.[87]

17-DMAG was developed by the NCI and Kosan as a more soluble analogue of 17-AAG. 17-DMAG can be formulated in 5% dextrose in water, is 50% orally bioavailable in mice,[25] and can also be administered iv. The maximum tolerated dose upon iv injection is 12 mg/m^2 (rats) and 8 mg/m^2 (dogs). In rats and dogs, the drug-related toxicities are gastrointestinal, hepatic, and bone-marrow related. Dogs also show signs of renal and gallbladder toxicities. The highest concentrations are found in the liver of rats, with progressively lower concentrations in the spleen, lung, and plasma. Only minimal amounts are found in the heart, and none is found in the brain.[88] 17-DMAG entered clinical trials in 2005, and showed 2 complete responses among 12 patients suffering of acute myeloid leukemia (AML).[89] Nevertheless, 17-DMAG was discontinued at the beginning of 2008.[35]

5.2. Purine 6. Purine **6** developed by Conforma Therapeutics and later by Biogen Idec was the first fully synthetic HSP90 inhibitor to reach the clinic (2005). In a fluorescent polarization assay, the binding affinity (K_i value) of **6** for HSP90α was 1.7 ± 0.4 nM, compared to 4.6 ± 0.5 nM for 17-AAG.[22] Purine **6** did not inhibit a panel of 10 kinases at 10 μM. In MCF7 cells, **6** degrades HER2 with an IC_{50} of 38 nM (Table 1) and induces the characteristic response of HSP90 inhibitors: degradation of HSP90 clients, up-regulation of HSP70, and no effect on PI3K, which is not a client of HSP90 (Figure 14).[22]

The mouse pharmacokinetic parameters were evaluated with an oral dose of **6** dissolved in 0.1 N HCl (100 mg/kg) (Table 4). Purine **6** was orally bioavailable and rapidly absorbed, peaking in the plasma after 0.1 h, with C_{max} = 31 μM. Purine **6** was rapidly cleared, with $T_{1/2}$ = 0.8 h. Despite the short half-life of **6** in serum, **6** was measurable in tumors at 24 and 48 h. More importantly, the pharmacological effect lasted for approximately 24 h. Just as with 17-AAG, the rapidly cleared **6** induced a durable pharmacodynamic response.

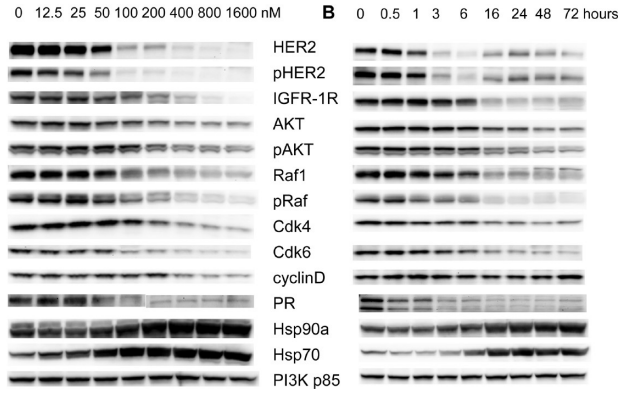

Figure 14. Effect of purine **6** on protein levels in MCF7 cells (A) as a function of concentration after 24 h and (B) as a function of time at 400 nM. Reprinted with permission from Lundgren, K.; Zhang, H.; Brekken, J.; Huser, N.; Powell, R. E.; Timple, N.; Busch, D. J.; Neely, L.; Sensintaffar, J. L.; Yang, Y.-C.; McKenzie, A.; Friedman, J.; Scannevin, R.; Kamal, A.; Hong, K.; Kasibhatla, S. R.; Boehm, M. F.; Burrows, F. J. BIIB021, an orally available, fully synthetic small molecule inhibitor of the heat shock protein HSP90. *Mol. Cancer Ther.* **2009**, *8*, 921−929, Figure 1.[22]

Table 4. Mouse Oral Pharmacokinetic Properties of Purine **6** Dosed at 100 mg/kg in 0.1 N HCl

compd	C_{max} [μM]	T_{max} [h]	AUC [μM·h]	$T_{1/2}$ [h]	HLM,[a] % parent remaining at 1 h
6	31	0.1	15	0.8	86

[a] Drug incubated for 1 h with human liver microsomes (HLM) at 37 °C.

For xenograft models, the human stomach carcinoma N87 tumor cell line was selected because of its relatively high HER2 expression. Tumor fragments were implanted subcutaneously, and treatment started once the tumor size reached 80−100 mm^3. Following oral dosing of **6** as a methanesulfonic acid salt at 125 mg/kg (equivalent to 96 mg/kg free base) on a 5-days/week schedule for 5 weeks, 87% tumor growth inhibition was observed (Table 5). Purine **6** was well tolerated exhibiting no treatment-related toxicity at these doses other than minimal weight loss (3−5%) over the course of the study. Purine **6** performed at least as well at 17-AAG (70% TGI, p = 0.02) given ip in PMSE[90] at 90 mg/kg. Decreasing the dose of **6** 4-fold led to an erosion of efficacy, with TGI ≈ 50% (Figure 15). Other tumors also responded well to **6** (Table 5).

5.3. Resorcinol 7. Resorcinol **7**, discovered by Vernalis and subsequently developed by Novartis, was the third fully synthetic inhibitor to reach clinic clinical trials (2007).[27,67,91−93] In a binding assay with the HSP90α and HSP90β isoforms, **7** demonstrated an IC_{50} of 7.8 and 21 nM, respectively (Table 1). The K_i values for HSP90α and HSP90β were found to be 9.0 and 8.2 nM, respectively. Resorcinol **7** demonstrated selectivity versus the HSP90 family members Grp94 (IC_{50} = 85 nM) and TRAP1 (IC_{50} = 535 nM) and was selective versus a panel of 13 kinases at 10 μM. In MCF7 cells, **7** degrades HER2 with an IC_{50} of 7 nM (Table 1) and inhibits the proliferation of 29 different human tumor cell lines, with GI_{50} values ranging from 2 to 40 nM. It is not a P-glycoprotein substrate.[27,67]

Table 5. Summary of Tumor Growth Inhibition with Purine **6**[a]

tumor model	dose (mg/kg)	weekly schedule	tumor type	% TGI	*p*
N87	125	qdx5	gastric	87	0.0001
BT474	120	qdx5	breast	94	0.00005
CWR22	120	qdx5	prostate	85	0.02
U87	75	bidx5	glioblastoma	70	0.02
SKOV3	124	qdx5	ovarian	67	0.003
Panc-1	124	qdx5	pancreatic	51	0.002

[a] qdx5 = daily, 5 days on and 2 days off. bidx5 = twice daily, 5 days on and 2 days off. Reprinted with permission from Lundgren, K.; Zhang, H.; Brekken, J.; Huser, N.; Powell, R. E.; Timple, N.; Busch, D. J.; Neely, L.; Sensintaffar, J. L.; Yang, Y.-C.; McKenzie, A.; Friedman, J.; Scannevin, R.; Kamal, A.; Hong, K.; Kasibhatla, S. R.; Boehm, M. F.; Burrows, F. J. BIIB021, an orally available, fully synthetic small molecule inhibitor of the heat shock protein HSP90. *Mol. Cancer Ther.* **2009**, *8*, 921−929, Table 2B.[22]

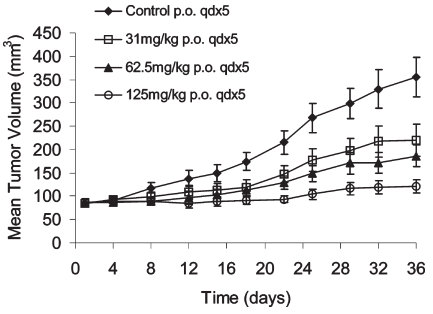

Figure 15. Growth of N87 tumor xenografts in athymic mice treated with purine **6** orally, 5 days/week. Reprinted with permission from Lundgren, K.; Zhang, H.; Brekken, J.; Huser, N.; Powell, R. E.; Timple, N.; Busch, D. J.; Neely, L.; Sensintaffar, J. L.; Yang, Y.-C.; McKenzie, A.; Friedman, J.; Scannevin, R.; Kamal, A.; Hong, K.; Kasibhatla, S. R.; Boehm, M. F.; Burrows, F. J. BIIB021, an orally available, fully synthetic small molecule inhibitor of the heat shock protein HSP90. *Mol. Cancer Ther.* **2009**, *8*, 921−929, Figure 2A.[22]

The percent parent remaining of **7** after being treated with mouse and human liver microsomes for 30 min was found to be 31% and 41%, respectively. The main metabolites identified in mouse plasma were the glucuronide, a deethylated product, likely the primary amide, and an oxidation product. However, the glucuronide is estimated to account for ∼95% of the plasma metabolites.[67]

In PK studies,[67] athymic mice bearing WM266.4 human melanoma xenografts were dosed iv with 50 mg/kg of **7**, formulated in DMSO/Tween-20/saline (10:5:85) (Table 6). The plasma AUC was 15 μM·h. The drug was rapidly cleared, with Cl = 143 mL/h (compared to the mouse liver blood flow of 108 mL/h) and $T_{1/2}$ = 1−2 h. However, as is observed with other HSP90 inhibitors, the compound showed increased concentrations in tumors and other tissues, with a ratio of the compound in tumor/plasma greater than 4. More importantly, **7** is cleared much more slowly from tumors, with an observed clearance of 20−40 mL/h and a half-life of 15 h. Intraperitoneal administration gave comparable parameters (Table 6), justifying the use of ip dosing in animal models.[67]

Regarding the pharmacodynamics, when mice with WM266.4 melanoma xenografts were treated with five daily ip doses (50 mg/kg) of **7**, a concentration range of 6.8−7.7 μM **7** in tumors was found over the 24 h period after the last dose. In addition the HSP90 clients HER2, p-ERK1/2, p-AKT, AKT, and HIF-1α were reduced versus controls

Table 6. Mouse PK Parameters of Resorcinol **7** Administered iv, 50 mg/kg

route	tissue	C_{max} [μM]	AUC [μM·h]	V_z [L]	Cl [L/h]	$T_{1/2}$ [h]
iv	plasma	49	15	0.875	0.143	1−2
iv	tumor	14	70	0.440	0.020	15
ip	plasma	53	26	0.077	0.082	1−2
ip	tumor	6	36	0.883	0.041	15

to 7−35%, 65−83%, 13−51%, 57−65%, and 60−85%, respectively. HSP70 was found to have increased by 247−281% of controls. The MTD for mice was 50 (mg/kg)/day. Increasing the dose to 70 (mg/kg)/day caused ∼10% body weight loss after day 8. With a 50 (mg/kg)/day dose given ip throughout the entire study a tumor growth inhibition of 46% was observed. In addition, **7** was tested in established colon, glioblastoma, breast, ovarian, and prostate xenografts and demonstrated a therapeutic response in all cases. Most notably, tumor regressions were observed in the BT474 high HER2 breast cancer model (5/12 tumors, TGI = 79%) and the U87MG glioblastoma model (average regressions of 58%).[67]

In a phase I/II trial, resorcinol **7** is administered intravenously as a 1 h infusion on a once a week schedule. The maximum dose reported to date is 54 mg/m^2. In general, asthenia/fatigue, nausea, and diarrhea were the most commonly reported adverse events. Reversible visual symptoms grades 1 and 2 were reported at 40 and 54 mg/m^2. Grade 3 dose-limiting toxicities were atrial flutter/fibrillation (1 of 12 patients at 22 mg/m^2), diarrhea (1 of 13 patients at 40 mg/m^2), anorexia combined with fatigue (1 of 13 patients at 40 mg/m^2), and asthenia (i.e., weakness, 1 of 9 patients at 54 mg/m^2).[94] At 40 mg/m^2, HSP70 was up-regulated 4−19 fold and a 20% reduction in soluble HER2 was achieved in 74% of patients.[95] Exploratory FDG-PET scans scans have demonstrated partial metabolic reponses in a number of patients, but no complete or partial response as per RECIST criteria has been reported in this study.[94]

5.4. Benzamides 8 and 9.[96,97] Benzamide **8**, a glycine prodrug of **9** originated at Serenex and developed by Pfizer, entered clinical trials in 2007. The reason for developing a prodrug was that **9** has a variable oral bioavailability, due at least in part to crystal polymorphism and poor solubility.[42]

In a FP-binding assay, **9** has a K_i of 1 nM, and in a cell-based HER2-degradation assay **9** has an IC_{50} of 20 nM (Table 1). Benzamide **9** also binds to Grp94 and TRAP1 but not to any other of the 2000 ATP-binding proteins contained in the Serenex platform. In a panel of breast, lung, and ovarian cancer cell lines, **9** inhibited cell proliferation with GI_{50} values ranging from 10 to 50 nM. In contrast to 17-AAG, the sensitivity of cancer cell lines to **9** in vitro did not correlate with the level of HER2 expression.[96] Benzamide **9** was also cytotoxic in drug-sensitive and drug-resistant multiple myeloma cell-lines with IC_{50} values of 19−186 nM at 48 h.[97] Thus, **9** proved to be potent in both HER2 driven (breast) and Akt driven (multiple myeloma) cell lines. In contrast, 17-AAG was less cytotoxic in multiple myeloma, with GI_{50} values of 100−500 nM.[97]

Benzamide **9** was administered to mice as its glycine prodrug **8** dissolved in 1% carboxymethyl cellulose and 0.5% Tween-80 at 10 mg/mL. Mice bearing human multiple myeloma MM.1S xenografts were treated with oral doses of 20 and 40 mg/kg on a 3×/week schedule, and **8** almost completely halted tumor growth. Results suggested that **8** inhibited cell growth and also acted on the bone

Table 7. Current Clinical Trials Involving HSP90 Inhibitors (July 2009)[a]

molecule	company	ROA	indications	phase
		Synthetic (Non-Geldanamycin Analogues)		
BIIB021	Biogen Idec	oral	GIST	II
			breast, CLL, solid tumors	I
SNX-5422	Serenex/Pfizer	oral	cancer	I
AV-142	Aveo	oral	cancer	I
MPC-3100	Myriad Genetics	oral	cancer	I
BIIB028	Biogen Idec	iv	cancer	I
AUY-922	Vernalis, Novartis	iv	breast, solid tumors	I
STA-9090	Synta	iv	cancer	I
KW-2478	Kyowa Hakko	iv	leukemia, multiple myeloma, CLL, NHL	I
AT-13387	Astex	iv	cancer	I
		17-AAG (Geldanamycin Analogues)		
KOS-953 (tanespimycin)	Kosan/BMS	iv	multiple myeloma	III
			breast, renal, thyroid, ovarian, pancreas	II
			pediactric solid tumors	I
IPI-504 (retaspimycin)	Infinity	iv	GIST	III
			NSCLC, breast	II
			sarcoma, multiple myeloma	I
IPI-493	Infinity	oral	solid tumors	I

[a] Source: ClinicalTrials.gov. Acronyms: GIST (gastrointestinal stromal tumor), CLL (chronic lymphocytic leukemia), NHL (non-Hodgkin's lymphoma), NSCLC (non-small-cell lung cancer).

Table 8. Summary of Preclinical Data: Cell-Based Potency, Half-Life in Mice (Plasma), and Typical Dosing Regimen To Observe Efficacy in Murine Xenograft Models

drug	company	HER2 [nM]	$T_{1/2}$ in mice [h]	typical dose regimen in mice
17-AAG	Kosan/BMS, Infinity	12	1	ip, 100 mg/kg, 3×/week
6	Biogen Idec	38	1	po, 100 mg/kg, 5×/week
7	Vernalis-Novartis	7	1	ip or iv, 30−50 mg/kg, (3−5)×/week
8	Serenex-Pfizer	20		po, 20−40 mg/kg, 3×/week
42	Serenex-Pfizer	20	~3	po, 50 mg/kg, 5×/week

marrow microenvironment by blocking osteoclastogenesis, a common complication of multiple myeloma, and angiogenesis.[97]

Pharmacokinetic data on **8**, the clinical prodrug of benzamide **9**, are not available. However, preclinical data have been published on SNX-5542 (**42**),[96] another prodrug of benzamide **9**. The structure of **42** has not been released. Also, the preclinical prodrug SNX-5542 should not be confused with the clinical prodrug SNX-5422. Prodrug **42** was formulated in 5% dextrose in water. Chronic treatment of mice with **42** at oral doses of 100 mg/kg or greater was associated with weight loss, and several mice died after 1 week of treatment, but **42** was well tolerated at a dose of 50 mg/kg, without weight loss or other gross toxicities. Judging from the published figure,[96] the active metabolite **9** has a plasma $T_{1/2} \approx 3$ h. Metabolite **9** accumulates preferentially in tumor tissues and has a longer half-life in tumors ($T_{1/2} \approx 10$ h). For instance, at 24 h, there was a >10-fold excess of drug found in tumor tissue (5 μM) compared with that in lung, small intestine, liver, skin, uterus, and kidney. The drug concentrations in muscle, brain, and heart were negligible (<0.1 μM) at this time point, a noteworthy point as cardiac toxicity has been a potential concern with this class of agents given the role played by chaperones in the maturation of the cardiac potassium channel hERG. Despite persistently high levels of metabolite **9** (1.8 μM) in the tumor, HER2 expression rose to baseline levels 48 h after dosing.[96]

In mice, at a dose of 50 mg/kg (five times per week), **42** caused ~50% tumor regressions in BT474 xenografts. The effect was durable, with no evidence of tumor regrowth noted 5 weeks after the last dose on day 35. In a H1650 xenograft, **42** did not cause regressions but still inhibited tumor growth (TGI ≈ 80%) and outperformed 17-AAG (TGI ≈ 30%, 100 mg/kg MWF).[96]

6. Conclusion

As mentioned earlier, there are 12 HSP90 inhibitors in clinical trials (Table 7), but the structures have been disclosed for only 6 of them: 17-AAG (quinone and hydroquinone forms), 17-DMAG, purine **6**, resorcinol **7**, and benzamide **8**. These six clinical inhibitors all have potencies on the order of 7−35 nM in a cell-based assay (Table 8) and half-lives of 1−3 h in the plasma of rodents. These inhibitors may distribute preferentially to the tumors and may have longer half-lives in the tumors than in the plasma, as in the case of 17-AAG and the active metabolite of **8**. In murine xenograft models, all compounds are required to be given at high doses (50−100 mg/kg) in order to achieve efficacy. Tumor growth can be inhibited, but regressions are rare and limited to the most sensitive cell-lines such as the high HER2 expressing BT474. In rodents, synergistic effects with paclitaxel have been published. The most advanced HSP90 inhibitors are 17-AAG and its hydroquinone **4**, currently in a phase III study in GIST, followed by purine **6**, entering phase II for the same indication. Clinical results have been published for 17-AAG, which is active in GIST as a single agent, in HER2 positive metastatic breast cancer in combination with trastuzumab, and in multiple myeloma in combination with bortezomib.

The field of HSP90 inhibition started 10 years ago and was pioneered by academic institutions. At that time the chances

of HSP90 inhibition leading to acceptable efficacy/safety margins were unclear. Small companies willing to take high risks followed on, and now a number of major pharmaceutical companies have HSP90 programs either via partnerships or acquisitions. One can expect ever more potent HSP90 inhibitors to emerge, with improved pharmacokinetic properties and possibly different tissue distributions. Nononcology indications may also emerge; besides cancer, the prevalent conditions mentioned in the literature with respect to HSP90 are Parkinson's disease, Alzheimer's disease, and fungal infections. For the time being, however, the focus is oncology. HSP90 inhibitors should not be expected to be magic bullets but should rather be viewed as an additional tool in the arsenal of the oncologist. Still, promising clinical results have been reported, and because HSP90 plays a role in so many pathways, HSP90 inhibitors are ideally suited for combination therapies. Moving forward, the challenge will be to design the best clinical trial, with the right combination and for the right indication.

Biographies

Marco A. Biamonte graduated from the Swiss Institute of Technology, Lausanne, Switzerland (1990). After completing a Ph.D. in total synthesis with Dr. Jim Staunton and Dr. Ian Paterson at the University of Cambridge, U.K. (1995), he performed postdoctoral studies in carbohydrate chemistry in the laboratories of Prof. Andrea Vasella at the Swiss Institute of Technology, Zurich, Switzerland (ETH-Z, 1998). Marco has worked as a medicinal chemist at Serono Pharmaceuticals, Conforma Therapeutics, and Biogen Idec. He is currently leading chemistry efforts on novel inhibitors of the heat shock protein 90.

Ryan Van de Water completed a B.S. at the University of California, San Diego, in 1998. He then received a Ph.D. from the University of California, Santa Barbara, with Dr. Thomas Pettus in 2003, where he worked on new synthetic methods and natural product synthesis. After completing postdoctoral research with Dr. Samuel Danishefsky in natural product synthesis, he joined Conforma Therapeutics in 2005, which was subsequently acquired by Biogen Idec. He is currently a medicinal chemist working on HSP90 inhibitors.

Joseph W. Arndt earned his Ph.D. in Chemistry from The Ohio State University where he studied reaction mechanisms of metalloproteins. He pursued postdoctoral studies in the laboratory of Professor Raymond Stevens at The Scripps Research Institute where he led structural and functional studies on botulinum neurotoxins. In 2006 he joined the Protein Crystallography Group at Biogen Idec, where he championed structural biology support for several biologic and small molecule programs including HSP90. His scientific interests include structure-based drug design, antibody engineering, and modulating protein−protein interactions.

Robert H. Scannevin graduated with a Ph.D. from the State University of New York at Stony Brook (1997). He completed his thesis project in the laboratory of Dr. James S. Trimmer, working on the molecular mechanisms of potassium channel localization. He went on to complete his postdoctoral training in the laboratory of Dr. Richard L. Huganir at Johns Hopkins University School of Medicine (2000) where he characterized novel glutamate receptor interacting molecules and their effects on subcellular trafficking. Robert has worked in molecular drug discovery since early 2001 for Wyeth, Johnson and Johnson, and Biogen Idec. He currently leads a biology research group focusing on discovering therapeutics for multiple sclerosis and Alzheimer's disease.

Daniel Perret received his M.B.A. from the Rady School of Management in 2006 and his M.S. in Bioengineering from the University of Technology at Compiegne, France. He joined Biogen Idec in 2001 as a Research Scientist and subsequently served as Senior Analyst, Market Research, and Area Business Manager from 2006 to 2008. Prior to joining Biogen Idec Daniel has worked in oncology research and development at Sanofi-Aventis and Genentech. He is currently leading the market research and competitive intelligence activities for the early stage oncology pipeline at Biogen Idec.

Wen-Cherng Lee graduated with a degree in Chemistry from the National Taiwan University in 1983 and remained as a full-time teaching assistant from 1985 to 1987. He completed his Ph.D. thesis under the guidance of Professor Stephen Martin at the University of Texas, Austin. After postdoctoral work with Professor Masamune at the Massachussetts Institute of Technology (MIT), Dr. Lee joined Biogen in 1993 and worked on several small-molecule drug discovery projects. Currently, he is an Associate Director in the medicinal chemistry department.

References

(1) Soo, E. T. L.; Yip, G. W. C.; Lwin, Z. M.; Kumar, S. D.; Bay, B.-H. Heat shock proteins as novel targets in cancer. *In Vivo* **2008**, *22*, 311–316.

(2) Pearl, L. H.; Prodromou, C. Structure and mechanism of the HSP90 molecular chaperone machinery. *Annu. Rev. Biochem.* **2006**, *75*, 271–294.

(3) This number is cited in several papers but without reference.

(4) Welch, W. J.; Feramisco, J. R. Purification of the major mammalian heat shock proteins. *J. Biol. Chem.* **1982**, *257*, 14949–14959.

(5) Messaoudi, S.; Peyrat, J. F.; Brion, J. D.; Alami, M. Recent advances in HSP90 inhibitors as antitumor agents. *Anti-Cancer Agents Med. Chem.* **2008**, *8*, 761–782.

(6) Sausville, E. A. Heat Shock Protein-90 Directed Therapeutics and Target Validation. In *Cancer Drug Design and Discovery*; Neidle, S., Ed.; Elsevier: Amsterdam, 2008; pp 336−350.

(7) (a) Dymock, B. W.; Drysdale, M. J.; McDonald, E.; Workman, P. Inhibitors of HSP90 and other chaperones for the treatment of cancer. *Expert Opin. Ther. Pat.* **2004**, *14*, 837–847. (b) Isaacs, J. S.; Wanping, X.; Neckers, L. Heat shock protein 90 as a molecular target for cancer therapeutics. *Cancer Cell* **2003**, *3*, 213–217. (c) Maloney, A.; Workman, P. HSP90 as a new therapeutic target for cancer therapy: the story unfolds. *Expert Opin. Biol. Ther.* **2002**, *2*, 3–24. (d) Richter, K.; Buchner, J. HSP90: chaperoning signal transduction. *J. Cell. Physiol.* **2001**, *188*, 281–290.

(8) Kamal, A.; Boehm, M. F.; Burrows, F. J. Therapeutic and diagnostic implications of HSP90 activation. *Trends Mol. Med.* **2004**, *10*, 283–290.

(9) Gorre, M. E.; Ellwood-Yen, K.; Chiosis, G.; Rosen, N.; Sawyers, C. L. BCR-ABL point mutants isolated from patients with imatinib mesylate-resistant chronic myeloid leukemia remain sensitive to inhibitors of the BCR-ABL chaperone heat shock protein 90. *Blood* **2002**, *100*, 3041–3044.

(10) Sawai, A.; Chandarlapaty, S.; Greulich, H.; Gonen, M.; Ye, Q.; Arteaga, C. L.; Sellers, W.; Rosen, N.; Solit, D. B. Inhibition of HSP90 down-regulates mutant epidermal growth factor receptor (EGFR) expression and sensitizes EGFR mutant tumors to Paclitaxel. *Cancer Res.* **2008**, *68*, 589–596.

(11) Kamal, A.; Thao, L.; Sensintaffar, J.; Zhang, L.; Boehm, M. F.; Fritz, L. C.; Burrows, F. J. A high-affinity conformation of HSP90 confers tumour selectivity on HSP90 inhibitors. *Nature* **2003**, *425*, 407–410.

(12) Workman, P. Altered states: selectively drugging the HSP90 cancer chaperone. *Trends Mol. Med.* **2004**, *10*, 47–51.

(13) Gooljarsingh, L. T.; Fernandes, C.; Yan, K.; Zhang, H.; Grooms, M.; Johanson, K.; Sinnamon, R. H.; Kirpatrick, R. B.; Kerrigan, J.; Lewis, T. A biochemical rationale for the anticancer effects of HSP90 inhibitors: slow, tight binding inhibition by geldanamycin and its analogues. *Proc. Natl. Acad. Sci. U.S.A.* **2006**, *103*, 7625–7630.

(14) Dickey, C. A.; Kamal, A.; Lundgren, K.; Klosak, N.; Bailey, R. M.; Dunmore, J.; Ash, P.; Shoraka, S.; Zlatkovic, J.; Eckman, C. B.; Patterson, C.; Dickson, D. W.; Nahman, N. S., Jr.; Hutton, M.; Burrows, F.; Petrucelli, L. The high-affinity HSP90-CHIP complex recognizes and selectively degrades phosphorylated tau client proteins. *J. Clin. Invest.* **2007**, *117*, 648–658.

(15) Roe, S. M.; Prodromou, C.; O'Brien, R.; Ladbury, J. E.; Piper, P. W.; Pearl, L. H. Structural basis for inhibition of the HSP90 molecular chaperone by the antitumor antibiotics radicicol and geldanamycin. *J. Med. Chem.* **1999**, *42*, 260–266.

(16) Stebbins, C. E.; Russo, A. A.; Schneider, C.; Rosen, N.; Hartl, F. U.; Pavletich, N. P. Crystal structure of an HSP90-geldanamycin complex: targeting of a protein chaperone by an antitumor agent. *Cell* **1997**, *89*, 239–250.
(17) Maroney, A. C.; Marugan, J. J.; Mezzasalma, T. M.; Barnakov, A. N.; Garrabrant, T. A.; Weaner, L. E.; Jones, W. J.; Barnakova, L. A.; Koblish, H. K.; Todd, M. J.; Masucci, J. A.; Deckman, I. C.; Galemmo, R. A., Jr.; Johnson, D. L. Dihydroquinone ansamycins: toward resolving the conflict between low in vitro affinity and high cellular potency of geldanamycin derivatives. *Biochemistry* **2006**, *45*, 5678–5685.
(18) Du, Y.; Moulick, K.; Rodina, A.; Aguirre, J.; Felts, S.; Dingledine, R.; Fu, H.; Chiosis, G. High-throughput screening fluorescence polarization assay for tumor-specific HSP90. *J. Biomol. Screening* **2007**, *12*, 915–924.
(19) Howes, R.; Barril, X.; Dymock, B. W.; Grant, K.; Northfield, C. J.; Robertson, A. G.; Surgenor, A.; Wayne, J.; Wright, L.; James, K.; Matthews, T.; Cheung, K. M.; McDonald, E.; Workman, P.; Drysdale, M. J. A fluorescence polarization assay for inhibitors of HSP90. *Anal. Biochem.* **2006**, *350*, 202–213.
(20) Kim, J.; Felts, S.; Llauger, L.; He, H.; Huezo, H.; Rosen, N.; Chiosis, G. Development of a fluorescence polarization assay for the molecular chaperone HSP90. *J. Biomol. Screening* **2004**, *9*, 375–381.
(21) Onuoha, S. C.; Mukund, S. R.; Coulstock, E. T.; Sengerova, B.; Shaw, J.; McLaughlin, S. H.; Jackson, S. E. Mechanistic studies on HSP90 inhibition by ansamycin derivatives. *J. Mol. Biol.* **2007**, *372*, 287–297.
(22) Lundgren, K.; Zhang, H.; Brekken, J.; Huser, N.; Powell, R. E.; Timple, N.; Busch, D. J.; Neely, L.; Sensintaffar, J. L.; Yang, Y.-C.; McKenzie, A.; Friedman, J.; Scannevin, R.; Kamal, A.; Hong, K.; Kasibhatla, S. R.; Boehm, M. F.; Burrows, F. J. BIIB021, an orally available, fully synthetic small molecule inhibitor of the heat shock protein HSP90. *Mol. Cancer Ther.* **2009**, *8*, 921–929.
(23) Schnur, R. C.; Corman, M. L.; Gallaschun, R. J.; Cooper, B. A.; Dee, M. F.; Doty, J. L.; Muzzi, M. L.; DiOrio, C. I.; Barbacci, E. G.; Miller, P. E.; Pollack, V. A.; Savage, D. M.; Sloan, D. E.; Pustilnik, L. R.; Moyer, J. D.; Moyer, M. P. erbB-2 oncogene inhibition by geldanamycin derivatives: synthesis, mechanism of action, and structure-activity relationships. *J. Med. Chem.* **1995**, *38*, 3813–3820.
(24) Ge, J.; Normant, E.; Porter, J. R.; Ali, J. A.; Dembski, M. S.; Gao, Y.; Georges, A. T.; Grenier, L.; Pak, R. H.; Patterson, J.; Sydor, J. R.; Tibbits, T. T.; Tong, J. K.; Adams, J.; Palombella, V. J. Design, synthesis, and biological evaluation of hydroquinone derivatives of 17-amino-17-demethoxygeldanamycin as potent, water-soluble inhibitors of HSP90. *J. Med. Chem.* **2006**, *49*, 4606–4615.
(25) Egorin, M. J.; Lagattuta, T. F.; Hamburger, D. R.; Covey, J. M.; White, K. D.; Musser, S. M.; Eiseman, J. L. Pharmacokinetics, tissue distribution and metabolism of 17-(dimethylaminoethylamino)-17-demethoxygeldanamycin (NSC 707545) in CD2F1 mice and Fischer 344 rats. *Cancer Chemother. Pharmacol.* **2002**, *49*, 7–19.
(26) Kasibhatla, S. R.; Hong, K.; Biamonte, M. A.; Busch, D. J.; Karjian, P. L.; Sensintaffar, J. L.; Kamal, A.; Lough, R. E.; Brekken, J.; Lundgren, K.; Grecko, R.; Timony, G. A.; Ran, Y.; Mansfield, R.; Fritz, L. C.; Ulm, E.; Burrows, F. J.; Boehm, M. F. Rationally designed high-affinity 2-amino-6-halopurine heat shock protein 90 inhibitors that exhibit potent antitumor activity. *J. Med. Chem.* **2007**, *50*, 2767–2778.
(27) Brough, P. A.; Aherne, W.; Barril, X.; Borgognoni, J.; Boxall, K.; Cansfield, J. E.; Cheung, K.-M. J.; Collins, I.; Davies, N. G. M.; Drysdale, M. J.; Dymock, B.; Eccles, S. A.; Finch, H.; Fink, A.; Hayes, A.; Howes, R.; Hubbard, R. E.; James, K.; Jordan, A. M.; Lockie, A.; Martins, V.; Massey, A.; Matthews, T. P.; McDonald, E.; Northfield, C. J.; Pearl, L. H.; Prodromou, C.; Ray, S.; Raynaud, F. I.; Roughley, S. D.; Sharp, S. Y.; Surgenor, A.; Walmsley, D. L.; Webb, P.; Wood, M.; Workman, P.; Wright, L. 4,5-Diarylisoxazole HSP90 chaperone inhibitors: potential therapeutic agents for the treatment of cancer. *J. Med. Chem.* **2008**, *51*, 196–218.
(28) (a) Huang, K. H.; Eaves, J.; Veal, J.; Barta, T.; Lifeng, G.; Hinkley, L.; Hanson, G. Tetrahydroindolone and Tetrahydroindazolone Derivatives. WO 2006/091963 **2006**. (b) Huang, K. H.; Eaves, J.; Veal, J.; Hall, S. E.; Barta, T. E.; Hanson, G. J. Cyclohexylamino Benzene, Pyridine, and Pyridazine Derivatives. US 2007/0207984, **2007**.
(29) (a) De Boer, C.; Meulman, P. A.; Wnuk, R. J.; Peterson, D. H. Geldanamycin, a new antibiotic. *J. Antibiot.* **1970**, *23*, 442–447. (b) De Boer, C.; Peterson, D. H. Antibiotic Geldanamycin. US 3595955, **1971**. (c) Gallaschun, R. J.; Moyer, M. P.; Schnur, R. C. Ansamycin Derivatives as Antioncogene and Anticancer Agents. WO 9501342, **1995**. (d) Whitesell, L.; Neckers, L.; Trepel, J.; Myers, C. Tumoricidal Activity of Benzoquinonoid Ansamycins against Prostate Cancer and Primitive Neural Malignancies. WO 9408578, **1994**.(e) Schulte, T. W.; Neckers, L. M. The benzoquinone ansamycin 17-allylamino-17-demethoxygeldanamycin binds to HSP90 and shares important biologic activities with geldanamycin. *Cancer Chemother. Pharmacol.* **1998**, *424*, 273–279.
(30) For a recent total synthesis: Qin, H.-L.; Panek, J. S. Total synthesis of the HSP90 inhibitor geldanamycin. *Org. Lett.* **2008**, *10*, 2477–2479.
(31) Rinehart, K. L.; Sasaki, K.; Slomp, G.; Grostic, M. F.; Olson, E. C.; Geldanamycin, I. Structure assignment. *J. Am. Chem. Soc.* **1970**, *92*, 7591–7593.
(32) Sasaki, K.; Inoue, Y. Geldanamycin Derivative and Antitumor Agent Containing It. DE 3006097, **1980**.
(33) Whitesell, L; Mimnaugh, E. G.; De Costa, B.; Myers, C. E.; Neckers, L. M. Inhibition of heat shock protein HSP90-pp60v-src heteroprotein complex formation by benzoquinone ansamycins: essential role for stress proteins in oncogenic transformation. *Proc. Natl. Acad. Sci. U.S.A.* **1994**, *91*, 8324–8328.
(34) Neckers, L.; Schulte, T. W.; Mimnaugh, E. Geldanamycin as a potential anticancer agent: its molecular target and biochemical activity. *Invest. New Drugs* **1999**, *17*, 361–373.
(35) Press Release, February 28, 2008: http://phx.corporate-ir.net/phoenix.zhtml?c=121014&p=irol-newsArticle&ID=1113760&highlight=.
(36) Chiosis, G.; Timaul, M. N.; Lucas, B.; Munster, P. N.; Zheng, F. F.; Sepp-Lorenzino, L.; Rosen, N. A small molecule designed to bind to the adenine nucleotide pocket of HSP90 causes Her2 degradation and the growth arrest and differentiation of breast cancer cells. *Chem. Biol.* **2001**, *8*, 289–299.
(37) Kasibhatla, S. R.; Hong, K.; Zhang, L.; Biamonte, M. A.; Boehm, M. F.; Shi, J.; Fan, J. Preparation of Purine Analogs as Heat Shock Protein 90 (HSP90) Inhibitors. WO 03/037860, **2003**.
(38) Biamonte, M. A.; Shi, J.; Hong, K.; Hurst, D. C.; Zhang, L.; Fan, J.; Busch, D. J.; Karjian, P. L.; Maldonado, A. A.; Sensintaffar, J. L.; Yang, Y.-C.; Kamal, A.; Lough, R. E.; Lundgren, K.; Burrows, F. J.; Timony, G. A.; Boehm, M. F.; Kasibhatla, S. R. Orally active purine-based inhibitors of the heat shock protein 90. *J. Med. Chem.* **2006**, *49*, 817–828.
(39) Zhang, L.; Fan, J.; Vu, K.; Hong, K.; Le Brazidec, J.-Y.; Shi, J.; Biamonte, M.; Busch, D. J.; Lough, R. E.; Grecko, R.; Ran, Y.; Sensintaffar, J. L.; Kamal, A.; Lundgren, K.; Burrows, F. J.; Mansfield, R.; Timony, G. A.; Ulm, E. H.; Kasibhatla, S. R.; Boehm, M. F. 7′-Substituted benzothiazolothio- and pyridinothiazolothio-purines as potent heat shock protein 90 inhibitors. *J. Med. Chem.* **2006**, *49*, 5352–5362.
(40) Llauger, L.; He, H.; Kim, J.; Aguirre, J.; Rosen, N.; Peters, U.; Davies, P.; Chiosis, G. Evaluation of 8-arylsulfanyl, 8- arylsulfoxyl, and 8-arylsulfonyl adenine derivatives as inhibitors of the heat shock protein 90. *J. Med. Chem.* **2005**, *48*, 2892–2905.
(41) Dymock, B. W.; Barril, X.; Brough, P. A.; Cansfield, J. E.; Massey, A.; McDonald, E.; Hubbard, R. E.; Surgenor, A.; Roughley, S. D.; Webb, P.; Workman, P.; Wright, L.; Drysdale, M. J. Novel, potent small-molecule inhibitors of the molecular chaperone HSP90 discovered through structure-based design. *J. Med. Chem.* **2005**, *48*, 4212–4215.
(42) Hall, S. Discovery and Pre-Clinical Profile of SNX-5422: An Orally Active Hsp90 Inhibitor in Phase 1 Trials for Solid and Hematological Tumors. Presented at the AACR Annual Meeting, **2008**; Abstract 2449.
(43) Cysyk, R. L.; Parker, R. J.; Barchi, J. J.; Steeg, P. S.; Hartman, N. R.; Strong, J. M. Reaction of geldanamycin and C17-substituted analogs with glutathione: product implications and pharmacological implications. *Chem. Res. Toxicol.* **2006**, *19*, 376–381.
(44) Yamaguchi, S.; Nakashima, T.; Kanda, Y. Preparation of Benzenoid Ansamycin Derivatives as HSP90 Family Protein Inhibitors for Treatment of Tumor. WO 2007/001049, **2007**.
(45) Zhang, M. Q.; Gaisser, S.; Nur-E-Alam, M.; Sheehan, L. S.; Vousden, W. A.; Gaitatzis, N.; Peck, G.; Coates, N. J.; Moss, S. J.; Radzom, M.; Foster, T. A.; Sheridan, R. M.; Gregory, M. A.; Roe, S. M.; Prodromou, C.; Pearl, L.; Boyd, S. M.; Wilkinson, B.; Martin, C. J. Optimizing natural products by biosynthetic engineering: discovery of nonquinone Hsp90 inhibitors. *J. Med. Chem.* **2008**, *51*, 5494–5497.
(46) Agatsuma, T.; Saitoh, Y.; Yamashita, Y.; Mizukami, T.; Akinaga, S.; Gomi, K.; Akasaka, K.; Takahashi, I. Preparation of Radicicol Derivatives as Tyrosine Kinase Inhibitors. WO 96/33989, **1996**.
(47) Ikuina, Y.; Amishiro, N.; Miyata, M.; Narumi, H.; Ogawa, H.; Akiyama, T.; Shiotsu, Y.; Akinaga, S.; Murakata, C. Synthesis and antitumor activity of novel *O*-carbamoylmethyloxime derivatives of radicicol. *J. Med. Chem.* **2003**, *46*, 2534–2541.

(48) Drysdale, M. J.; Brough, P. A. Medicinal chemistry of HSP90 inhibitors. *Curr. Top. Med. Chem.* **2008**, *8*, 859–868.
(49) Shiau, A. K.; Harris, S. F.; Southworth, D. R.; Agard, D. A Structural analysis of *E. coli* hsp90 reveals dramatic nucleotide-dependent conformational rearrangements. *Cell* **2006**, *127*, 329–340.
(50) Ali, M. M.; Roe, S. M.; Vaughan, C. K.; Meyer, P.; Panaretou, B.; Piper, P. W.; Prodromou, C.; Pearl, L. H. Crystal structure of an HSP90-nucleotide-p23/Sba1 closed chaperone complex. *Nature* **2006**, *440*, 1013–1017.
(51) Dollins, D. E.; Warren, J. J.; Immormino, R. M.; Gewirth, D. T. Structures of GRP94-nucleotide complexes reveal mechanistic differences between the hsp90 chaperones. *Mol. Cell* **2007**, *28*, 41–56.
(52) Wandinger, S. K.; Richter, K.; Buchner, J. The HSP90 chaperone machinery. *J. Biol. Chem.* **2008**, *283*, 18473–18477.
(53) Prodromou, C.; Roe, S. M.; O'Brien, R.; Ladbury, J. E.; Piper, P. W.; Pearl, L. H. Identification and structural characterization of the ATP/ADP-binding site in the HSP90 molecular chaperone. *Cell* **1997**, *90*, 65–75.
(54) Meyer, P.; Prodromou, C.; Hu, B.; Vaughan, C.; Roe, S. M.; Panaretou, B.; Piper, P. W.; Pearl, L. H. Structural and functional analysis of the middle segment of hsp90: implications for ATP hydrolysis and client protein and cochaperone interactions. *Mol. Cell* **2003**, *11*, 647–658.
(55) Sato, S.; Fujita, N.; Tsuruo, T. Modulation of Akt kinase activity by binding to HSP90. *Proc. Natl. Acad. Sci. U.S.A.* **2000**, *97*, 10832–10837.
(56) Harris, S. F.; Shiau, A. K.; Agard, D. A. The crystal structure of the carboxy-terminal dimerization domain of htpG, the *Escherichia coli* HSP90, reveals a potential substrate binding site. *Structure* **2004**, *12*, 1087–1097.
(57) Minami, Y.; Kimura, Y.; Kawasaki, H.; Suzuki, K.; Yahara, I. The carboxy-terminal region of mammalian HSP90 is required for its dimerization and function in vivo. *Mol. Cell. Biol.* **1994**, *14*, 1459–1464.
(58) Richter, K.; Moser, S.; Hagn, F.; Friedrich, R.; Hainzl, O.; Heller, M.; Schlee, S.; Kessler, H.; Reinstein, J.; Buchner, J. Intrinsic inhibition of the HSP90 ATPase activity. *J. Biol. Chem.* **2006**, *281*, 11301–11311.
(59) Wegele, H.; Muller, L.; Buchner, J. Hsp70 and HSP90, a relay team for protein folding. *Rev. Physiol. Biochem. Pharmacol.* **2004**, *151*, 1–44.
(60) Onuoha, S. C.; Coulstock, E. T.; Grossmann, J. G.; Jackson, S. E. Structural studies on the co-chaperone Hop and its complexes with HSP90. *J. Mol. Biol.* **2008**, *379*, 732–744.
(61) Ballinger, C. A.; Connell, P.; Wu, Y.; Hu, Z.; Thompson, L. J.; Yin, L. Y.; Patterson, C. Identification of CHIP, a novel tetratricopeptide repeat-containing protein that interacts with heat shock proteins and negatively regulates chaperone functions. *Mol. Cell. Biol.* **1999**, *19*, 4535–4545.
(62) Connell, P.; Ballinger, C. A.; Jiang, J.; Wu, Y.; Thompson, L. J.; Hohfeld, J.; Patterson, C. The co-chaperone CHIP regulates protein triage decisions mediated by heat-shock proteins. *Nat. Cell Biol.* **2001**, *3*, 93–96.
(63) Meacham, G. C.; Patterson, C.; Zhang, W.; Younger, J. M.; Cyr, D. M. The Hsp70 co-chaperone CHIP targets immature CFTR for proteasomal degradation. *Nat. Cell Biol.* **2001**, *3*, 100–105.
(64) Murata, S.; Minami, Y.; Minami, M.; Chiba, T.; Tanaka, K. CHIP is a chaperone-dependent E3 ligase that ubiquitylates unfolded protein. *EMBO Rep.* **2001**, *2*, 1133–1138.
(65) Dai, Q.; Zhang, C.; Wu, Y.; McDonough, H.; Whaley, R. A.; Godfrey, V.; Li, H. H.; Madamanchi, N.; Xu, W.; Neckers, L.; Cyr, D.; Patterson, C. CHIP activates HSF1 and confers protection against apoptosis and cellular stress. *EMBO J.* **2003**, *22*, 5446–5458.
(66) Obermann, W. M. J.; Sondermann, H.; Russo, A. A.; Pavletich, N. P.; Hartl, F. U. In vivo function of HSP90 is dependent on ATP binding and ATP hydrolysis. *J. Cell Biol.* **1998**, *143*, 901–910.
(67) Eccles, S. A.; Massey, A.; Raynaud, F. I.; Sharp, S. Y.; Box, G.; Valenti, M.; Patterson, L.; Brandon, A. D.; Gowan, S.; Boxall, F.; Aherne, W.; Rowlands, M.; Hayes, A.; Martins, V.; Urban, F.; Boxall, K.; Prodromou, C.; Pearl, L.; James, K.; Matthews, T. P.; Cheung, K. M.; Kalusa, A.; Jones, K.; McDonald, E.; Barril, X.; Brough, P. A.; Cansfield, J. E.; Dymock, B.; Drysdale, M. J.; Finch, H.; Howes, R.; Hubbard, R. E.; Surgenor, A.; Webb, P.; Wood, M.; Wright, L.; Workman, P. NVP-AUY922: a novel heat shock protein 90 inhibitor active against xenograft tumor growth, angiogenesis, and metastasis. *Cancer Res.* **2008**, *68*, 2850–2860.
(68) Barta, T. E.; Veal, J. M.; Rice, J. W.; Partridge, J. M.; Fadden, R. P.; Ma, W.; Jenks, M.; Geng, L. F.; Hanson, G. J.; Huang, K. H.; Barabasz, A. F.; Foley, B. E.; Otto, J.; Hall, S. E. Discovery of benzamide tetrahydro-4*H*-carbazol-4-ones as novel small molecule inhibitors of HSP90. *Bioorg. Med. Chem. Lett.* **2008**, *18*, 3517–3521.
(69) Wright, L.; Barril, X.; Dymock, B.; Sheridan, L.; Surgenor, A.; Beswick, M.; Drysdale, M.; Collier, A.; Massey, A.; Davies, N.; Fink, A.; Fromont, C.; Aherne, W.; Boxall, K.; Sharp, S.; Workman, P.; Hubbard, R. E. Structure−activity relationships in purine-based inhibitor binding to HSP90 isoforms. *Chem. Biol.* **2004**, *11*, 775–785.
(70) Fritz, C. C.; Ge, J.; Hafeez, N.; Tillotson, B., Depew, K.; Coco, J.; Basuki, J.; Lim, A.; Patterson, J.; Porter, J. R. ; Palombella, V.; Normant, E. (Infinity Pharmaceuticals) Comparison of the Cellular and Biochemical Properties of Ansamycin and Non-Ansamycin Based Inhibitors. Presented at the AACR-EORTC Meeting, Geneva, **2008**.
(71) McCollum, A. K.; TenEyck, C. J.; Stensgard, B.; Morlan, B. W.; Ballman, K. V.; Jenkins, R. B.; Toft, D. O.; Erlichman, C. P-Glycoprotein-mediated resistance to HSP90-directed therapy is eclipsed by the heat shock response. *Cancer Res.* **2008**, *68*, 7419–7427.
(72) (a) Nguyen, D. M.; Chen, A.; Mixon, A.; Schrump, D. S. Sequence-dependent enhancement of paclitaxel toxicity in non-small cell lung cancer by 17-allylamino 17-demethoxygeldanamycin. *J. Thorac. Cardiovasc. Surg.* **1999**, *118*, 908–915. (b) Nguyen, D. M.; Lorang, D.; Chen, G. A.; Stewart, J. H.; Tabibi, E.; Schrump, D. S. Enhancement of paclitaxel-mediated cytotoxicity in lung cancer cells by 17-allylamino geldanamycin: in vitro and in vivo analysis. *Ann. Thorac. Surg.* **2001**, *72*, 371–378. (c) Sain, N.; Krishnan, B.; Ormerod, M. G.; De Rienzo, A.; Liu, W. M.; Kaye, S. B.; Workman, P.; Jackman, A. L. Potentiation of paclitaxel activity by the HSP90 inhibitor 17-allylamino-17-demethoxygeldanamycin in human ovarian carcinoma cell lines with high levels of activated AKT. *Mol. Cancer Ther.* **2006**, *5*, 1197–1208.
(73) Solit, D. B.; Basso, A. D.; Olshen, A. B.; Scher, H. I.; Rosen, N. Inhibition of heat shock protein 90 function down-regulates Akt kinase and sensitizes tumors to taxol. *Cancer Res.* **2003**, *63*, 2139–2144.
(74) McCollum, A. K.; Lukasiewicz, K. B.; TenEyck, C. J.; Lingle, W. L.; Toft, D. O.; Erlichman, C. Cisplatin abrogates the geldanamycin-induced heat shock response. *Mol. Cancer Ther.* **2008**, *7*, 3256–3264.
(75) Duus, J.; Bahar, H. I.; Venkataraman, G.; Ozpuyan, F.; Izban, K. F.; Al-Masri, H.; Maududi, T.; Toor, A.; Alkan, S. Analysis of expression of heat shock protein-90 (HSP90) and the effects of HSP90 inhibitor (17-AAG) in multiple myeloma. *Leuk. Lymphoma* **2006**, *47*, 1369–1378.
(76) Raja, S. M.; Clubb, R. J.; Bhattacharyya, M.; Dimri, M.; Cheng, H.; Pan, W.; Ortega-Cava, C.; Lakku-Reddi, A.; Naramura, M.; Band, V.; Band, H. A combination of trastuzumab and 17-AAG induces enhanced ubiquitinylation and lysosomal pathway-dependent ErbB2 degradation and cytotoxicity in ErbB2-overexpressing breast cancer cells. *Cancer Biol. Ther.* **2008**, *7*, 1630–1640.
(77) Banerji, U.; Walton, M.; Raynaud, F.; Grimshaw, R.; Kelland, L.; Valenti, M.; Judson, I.; Workman, P. Pharmacokinetic−pharmacodynamic relationships for the heat shock protein 90 molecular chaperone inhibitor 17-allylamino, 17-demethoxygeldanamycin in human ovarian cancer xenograft models. *Clin. Cancer. Res.* **2005**, *11*, 7023–7032.
(78) (a) Solit, D. B.; Chiosis, G. Development and application of HSP90 inhibitors. *Drug Discovery Today* **2008**, *13*, 38–43. (b) Taldone, T.; Gozman, A.; Maharaj, R.; Chiosis, G. Targeting HSP90: small-molecule inhibitors and their clinical development. *Curr. Opin. Pharmacol.* **2008**, *8*, 370–374.
(79) Solit, D. B.; Percy, I.; Kopil, C.; Sikorski, R.; Morris, M. J.; Slovin, S. F.; Kelly, W. K.; DeLaCruz, A.; Curley, T.; Heller, G.; Larson, S.; Schwartz, L.; Egorin, M. J.; Rosen, N.; Scher, H. I. Phase I trial of 17-allylamino-17-demethoxygeldanamycin in patients with advanced cancer. *Clin. Cancer. Res.* **2007**, *13*, 1775–1782.
(80) Banerji, U.; O'Donnell, A.; Scurr, M.; Pacey, S.; Stapleton, S.; Asad, Y.; Simmons, L.; Maloney, A.; Raynaud, F.; Campbell, M.; Walton, M; Lakhani, S.; Kaye, S.; Workman, P.; Judson, I. Phase I pharmacokinetic and pharmacodynamic study of 17-allylamino,17-demethoxygeldanamycin in patients with advanced malignancies. *J. Clin. Oncol.* **2005**, *23*, 4152–4161.
(81) 30% propylene glycol, 20% cremophor EL, 50% ethanol to a concentration of 10 mg/mL in the vial, 200 mg/vial.
(82) Modi, S.; Stopeck, A. T.; Gordon, M. S.; Mendelson, D.; Solit, D. B.; Bagatell, R.; Ma, W.; Wheler, J.; Rosen, N.; Norton, L.; Cropp, G. F.; Johnson, R. G.; Hannah, A. L.; Hudis, C. A. Combination of trastuzumab and tanespimycin (17-AAG, KOS-953) is safe and active in trastuzumab-refractory HER-2-overexpressing breast cancer. A dose-escalation study. *J. Clin. Oncol.* **2007**, *25*, 5410–5417.

(83) 48th ASH Meeting, Orlando, FL, December 2006.
(84) http://clinicaltrial.gov/ct/show/NCT00319930.
(85) Sydor, J. R.; Normant, E.; Pien, C. S.; Porter, J. R.; Ge, J.; Grenier, L.; Pak, R. H.; Ali, J. A.; Dembski, M. S.; Hudak, J.; Patterson, J.; Penders, C.; Pink, M.; Read, M. A.; Sang, J.; Woodward, C.; Zhang, Y.; Grayzel, D. S.; Wright, J.; Barrett, J. A.; Palombella, V. J.; Adams, J.; Tong, J. K. Development of 17-allylamino-17-demethoxygeldanamycin hydroquionone hydrochloride (IPI-504), an anti-cancer agent directed against HSP90. *Proc. Natl. Acad. Sci. U.S.A.* **2006**, *103*, 17408–17413.
(86) Presented at the ASCO Annual Meeting, **2007**.
(87) Infinity Press Release, April 15, **2009**.
(88) Glaze, E. R.; Lambert, A. L.; Smith, A. C.; Page, J. G.; Johnson, W. D.; McCormick, D. L.; Brown, A. P.; Levine, B. S.; Covey, J. M.; Egorin, M. J.; Eiseman, J. L.; Holleran, J. L.; Sausville, E. A.; Tomaszewski, J. E. Preclinical toxicity of a geldanamycin analog, 17-(dimethylaminoethylamino)-17-demethoxygeldanamycin (17-DMAG), in rats and dogs: potential clinical relevance. *Cancer Chemother. Pharmacol.* **2005**, *56*, 637–647.
(89) Lancet, J.; Gojo, I.; Baer, M.; Burton, M.; Klein, M.; Nowadly, C.; Gorre, M.; Zhong, Z.; Johnson, R. G.; Hannah, A. L. Phase 1, Pharmacokinetic (PK) and Pharmacodynamic (PD) Study of of the Hsp-90 Inhibitor, KOS-1022 (17-DMAG), in Patients with Refractory Hematological Malignancies. Presented at the ASCO Annual Meeting, **2006**; Abstract 2081.
(90) P = phospholipon 90G (phospholipid surfactant). M = miglyol 812N (short chain triglyceride). S = soybean oil (long chain triglyceride). E = emulsion.
(91) Cheung, K. J.; Matthews, T. P.; James, K.; Rowlands, M. G.; Boxall, K. J.; Sharp, S. Y.; Maloney, A.; Roe, S. M.; Prodromou, C.; Pearl, L. H.; Aherne, G. W.; McDonald, E.; Workman, P. The identification, synthesis, protein crystal structure and in vitro biochemical evaluation of a new 3,4-diarylpyrazole class of HSP90 inhibitors. *Bioorg. Med. Chem. Lett.* **2005**, *15*, 3338–3343.
(92) Sharp, S. Y.; Prodromou, C.; Boxall, K.; Powers, M. V.; Holmes, J. L.; Box, G.; Matthews, T. P.; Cheung, K. J.; Kalusa, A.; James, K.; Hayes, A.; Hardcastle, A.; Dymock, B.; Brough, P. A.; Barril, X.; Cansfield, J. E.; Wright, L.; Surgenor, A.; Foloppe, N.; Hubbard, R. E.; Aherne, W.; Pearl, L.; Jones, K.; McDonald, E.; Raynaud, F.; Eccles, S.; Drysdale, M.; Workman, P. Inhibition of the heat shock protein 90 molecular chaperone in vitro and in vivo by novel, synthetic, potent resorcinylic pyrazole/isoxazole amide analogues. *Mol. Cancer Ther.* **2007**, *6*, 1198–1211.
(93) Jensen, M. R.; Schoepfer, J.; Radimerski, T.; Massey, A.; Guy, C. T.; Brueggen, J.; Quadt, C.; Buckler, A.; Cozens, R.; Drysdale, M. J.; Garcia-Echeverria, C.; Chene, P. NVP-AUY922: a small molecule HSP90 inhibitor with potent antitumor activity in preclinical breast cancer models. *Breast Cancer Res.* **2008**, *10*, R33 (12 pages) .
(94) Sessa, C.; Sharma, S.; Britten, C.; Vogelzang, N.; Bhalla, K.; Mita, M.; Pluard, T.; Stiegler, P.; Quadt, C.; Shapiro, G. I. A Phase I Dose-Escalation Study of AUY922, a Novel HSP90 Inhibitor, in Patients with Advanced Solid Malignancies. Presented at the ASCO Annual Meeting, **2009**; Abstract 3532.
(95) Ida, S.; Motwani, M.; Jensen, M.; Wang, J.; Huseinovic, N.; Stiegler, P.; Wang, X.; Quadt, C. Pharmacodynamics and Pharmacokinetics of AUY922 in a Phase I/II Study of Patients with Solid Tumors. Presented at the ASCO Annual Meeting, **2009**; Abstract 3533.
(96) Chandarlapaty, S.; Sawai, A; Ye, Q.; Scott, A.; Silinski, M.; Huang, K.; Fadden, P.; Partridge, J.; Hall, S.; Steed, P.; Norton, L.; Rosen, N.; Solit, D. B. SNX2112, a synthetic heat shock protein 90 inhibitor, has potent antitumor activity against HER kinase-dependent cancers. *Clin. Cancer Res.* **2008**, *14*, 240–248.
(97) Okawa, Y.; Hideshima, T.; Steed, P.; Vallet, S.; Hall, S.; Huang, K.; Rice, J.; Barabasz, A.; Foley, B.; Ikeda, H.; Raje, N.; Kiziltepe, T.; Yasui, H.; Enatsu, S.; Anderson, K. C. SNX-2112, a selective Hsp90 inhibitor, potently inhibits tumor cell growth, angiogenesis, and osteoclastogenesis in multiple myeloma and other hematologic tumors by abrogating signaling via Akt and ERK. *Blood* **2009**, *113*, 846–855.